

Received June 9, 2020, accepted June 15, 2020, date of publication June 17, 2020, date of current version June 30, 2020.

Digital Object Identifier 10.1109/ACCESS.2020.3003253

Analysis of Temperature Profiles in Longitudinal Fin Designs by a Novel Neuroevolutionary Approach

ASHFAQ AHMAD¹, MUHAMMAD SULAIMAN¹, AHMAD ALHINDI^{2,3}, (Member, IEEE),
AND ABDULAH JEZA ALJOHANI^{4,5}, (Member, IEEE)

¹Department of Mathematics, Abdul Wali Khan University at Mardan, Mardan 23200, Pakistan

²Department of Computer Science, Umm Al-Qura University, Makkah 21955, Saudi Arabia

³Center of Innovation and Development in AI (CIADA), Umm Al-Qura University, Makkah 21955, Saudi Arabia

⁴Department of Electrical and Computer Engineering, King Abdulaziz University, Jeddah 21589, Saudi Arabia

⁵Center of Excellence in Intelligent Engineering Systems, King Abdulaziz University, Jeddah 21589, Saudi Arabia

Corresponding author: Muhammad Sulaiman (msulaiman@awkum.edu.pk)


This work was supported by the Deanship of Scientific Research at Umm Al-Qura University under Grant 19-COM-1-01-0022.

ABSTRACT Real application problems in physics, engineering, economics, and other disciplines are often modeled as differential equations. Classical numerical techniques are computationally expensive when we require solutions to our mathematical problems with no prior information. Hence, researchers are more interested in developing numerical methods that can obtain better solutions with fewer efforts and computational time. Heuristic algorithms are considered suitable candidates for such type of problems. In this research, we have developed a new neuroevolutionary algorithm that combines the power of feed-forward artificial neural networks (ANNs) and a modern metaheuristic, the Symbiotic Organism Search (SOS) algorithm. With our new approach, we have analyzed the simultaneous surface convection and radiation during heat transfer in different models of fins/ heat exchangers. Longitudinal fins are considered with concave parabolic, rectangular and trapezoidal shapes. We have analyzed our problem in two scenarios and six sub-cases. Our solutions are of high quality, with minimum residual errors in all cases. We have established the quality of our results by calculating values of different performance indicators like Root-mean-square error (RMSE), Absolute error (AE), Generational distance (GD), Mean absolute deviation (MAD), Nash–Sutcliffe efficiency (NSE), Error in Nash–Sutcliffe efficiency (ENSE). Statistical and graphical analysis of our results suggests that our approach is suitable for handling real application problems. We have compared our results with state-of-the-art results, and the outcome of our analysis points to the superiority of our approach.

INDEX TERMS Approximate solutions, artificial neural networks, heat transfer analyses, longitudinal fins, metaheuristics, symbiotic organism search optimizer.

I. INTRODUCTION

Differential equations are essential to model many of the physical, economic, and engineering problems. Many publications have appeared in literature by considering solutions to the differential equations using classical numerical and analytical techniques. Scientists and engineers are continuously studying the existing and new methods for solving differential equations (DEs). Real-life problems often involve singular, nonlinear, and higher-order ordinary differential equations (ODEs).

The associate editor coordinating the review of this manuscript and approving it for publication was Shiping Wen .

Classical and analytical approaches are not efficient in obtaining solutions to ODEs. Therefore, new approximate techniques are used to obtain better approximate solutions to complex problems. Many solution techniques are designed and implemented to solve design engineering problems, such as the homotopy analysis method (HAM) [1], the method of bilaterally bounded (MBB) [2], the variational iteration method (VIM) [3], [4], and the modified Adomian decomposition method (ADM) [5], [6].

Zhou [7] introduced the differential transform method (DTM), in which Taylor series solutions are used to get approximate solutions of ODEs. DTM is widely used to solve initial value problems and many nonlinear design engineering

problems [8]–[11]. In recent studies, DTM is hybridized with the finite difference method and is used for solving ODEs. Approximate solutions for different problems are reported in [12]–[14]. Other approximate techniques, including hybrids of homotopy perturbation method, Variational iterative method, DTM, and Padé approximation technique, are developed to overcome the weaknesses of its earlier versions [15].

Many researchers have attempted to solve linear and nonlinear differential and integro-differential equations by using approximate methods [16]–[20]. However, all these methods are problem-specific and do not apply to every problem. Hence, in the case of design engineering problems, these techniques fail to get solutions of good quality.

In literature, there are many techniques for solving ODEs, but none of these techniques fulfills all requirements of engineers. In design engineering, most of the problems contain highly nonlinear and complex ODEs. Researchers are continuously developing numerical methods that can solve ODEs with arbitrary boundaries and initial points. For instance, DTM was applied to solve the Glauert-jet Problem [11], but results were not accurate. Moreover, VIM and HPM techniques failed to obtain results for kinematics of a particle in fluids. It was observed that this failure was due to their parameter-dependent nature [21], [22]. All techniques discussed so far are collectively called classical methods.

Therefore, metaheuristic techniques are better alternatives, which are capable of solving differential equations in less time and can obtain better results. Among these techniques, Nature-inspired algorithms are considered as best solvers. These techniques are simulating Natural phenomena and are frequently applied to solve real application problems, and near-optimal results are found [23]–[26].

Recently, numerous applications of Nature-inspired algorithms appeared in literature [27]–[33]. These techniques are used to obtain solutions to optimization problems involving ODEs and nonlinear complex objective functions. Cuckoo search (CS) algorithm is used to find design solutions to porous fin problems [30]. The Whale optimization algorithm (WOA) is applied to find the optimal design of plate-fin heat exchangers [31]. The plant propagation algorithm (PPA) is implemented to solve design engineering problems [34], [35], and the optimization problem of optimal operation of directional overcurrent relays is studied in [36]. A theoretical analysis of PPA is discussed with details in [37]. A hybrid soft computing technique combining the artificial neural networks and fractional-order DPSO algorithm is applied to analyze the corneal shape model of eye surgery [28]. A neuroevolutionary approach is used to analyze the oscillatory behavior of heart [27].

Nowadays, mathematical models of real applications are represented as ODEs and different metaheuristics are been designed to solve these problems. Numerical optimization techniques like genetic algorithm [38], [39], different variants of particle swarm optimization (PSO) [40]–[42], interior point algorithm [43], evolutionary programming [44]

and others [45], [46] are used to solve mathematical models involving ODEs and PDEs. In [41], a variant of PSO is designed and applied to solve nonlinear ODEs.

Soft computing techniques are applied to generate visible videos from raw footage, which has many applications, like, video compression, movie production, slow-motion filming, video surveillance, and forensic analysis [47]. A sparse, fully convolutional network (FCN) is proposed for face labeling. The problem of substantial redundancy in parameters and connections is resolved with the help of FCN [48]. An improved version of FCN is designed to solve the face labeling problem [49]. A synchronization issue related to delayed memristive neural networks (MNNs), including leakage delay and parameter variations via event-triggered control, is studied in [50]. Another critical aspect of synchronization in multiple MNNs with cyber-physical attacks through distributed event-triggered control is considered in [51].

Recently, single layer Chebyshev ANNs with regression-based weights are used to present solutions to ODEs [52]. A new approach is recently introduced in [53], and Lane–Emden (LE) equations are solved. The genetic algorithm (GAs) and the Interior-point algorithm (IPA) are used as dual optimizers. This approach makes the process slow and consumes a higher number of function evaluations and computational resources by both algorithms. These solutions involve unknown design weights, and activation functions like log-sigmoid function, radial basis function, hyperbolic functions, and Morlet wavelet function [53], [54]. This issue has inspired the authors of this manuscript to design a well balanced single optimizer based efficient soft computing procedure for calculating these unknown weights and obtain high-quality solutions to real application problems involving ODEs. Fitness functions are designed to evaluate the fitness of each candidate solution. These functions are minimized by efficient metaheuristic the SOS-algorithm. We have analyzed two scenarios and six sub-cases of a real application problem related to fin heat transfer [55]. We have analyzed the heat transfer in fins by looking at simultaneous surface convection and radiation in different models of fins. Longitudinal fins are considered with concave parabolic, rectangular and trapezoidal shapes; see FIGURE (2).

Our key contributions are given as follows:

- A new soft computing procedure is designed by combining ANNs and an efficient metaheuristic the Symbiotic Organism Search (SOS) algorithm, and it is named as ANN-SOS algorithm, see FIGURES (1) and (3).
- Designs of longitudinal fins (heat exchangers) are analyzed for heat transfer by looking at their concave parabolic, rectangular and trapezoidal shapes; see FIGURE (2).
- Mathematical model of longitudinal fins is derived, and the problem is solved and analyzed by using the ANN-SOS algorithm for rectangular, trapezoidal, and concave parabolic shapes.

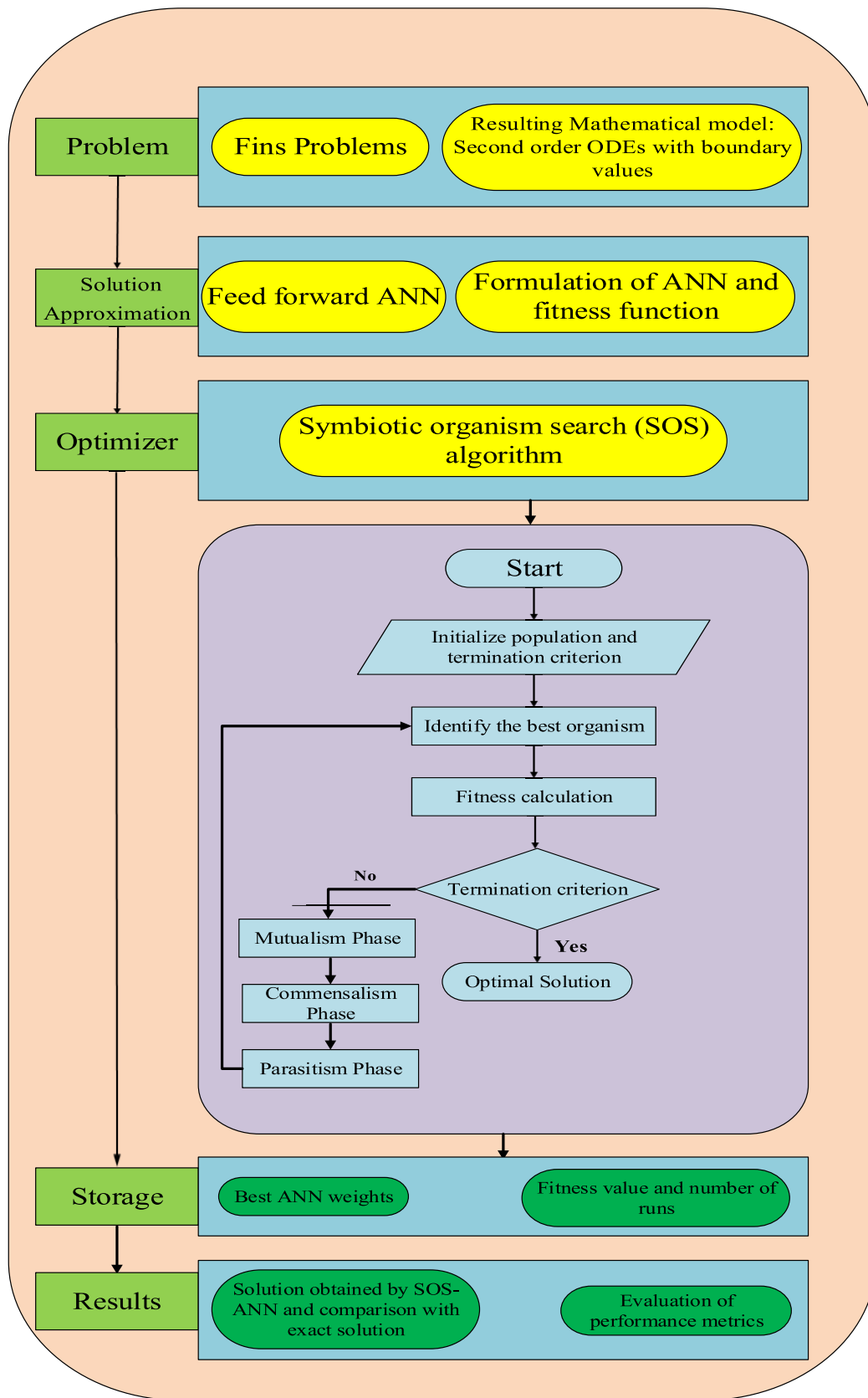


FIGURE 1. Graphical abstract of our neuroevolutionary approach.

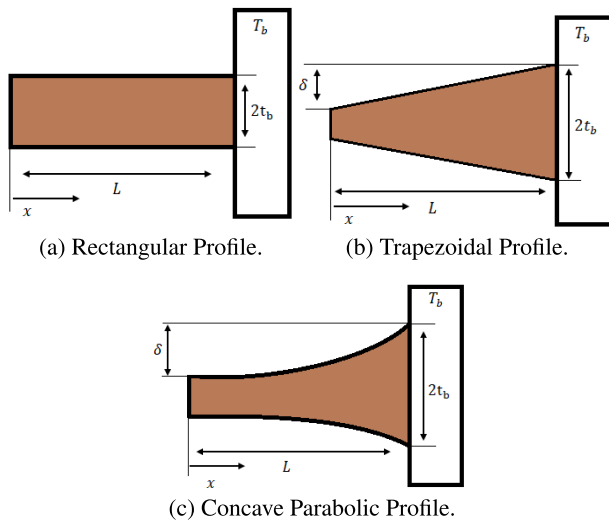


FIGURE 2. Different longitudinal fin shapes considered in this study.

- To validate the mathematical model and the ANN-SOS algorithm, we have considered two main scenarios with six sub-problems, see FIGURE (4).
- Performance indicators are used to evaluate the quality of our solutions and the efficiency of our soft computing approach the ANN-SOS procedure. Values of Root mean squared errors (RMSE), Absolute errors (AE), Generational distance (GD), Mean absolute deviation (MAD), Nash-Sutcliffe efficiency (NSE), Error in Nash-Sutcliffe efficiency ENSE) are calculated for all six sub-problems to validate the mathematical model and assure that we have obtained the best solutions through our procedure.

This paper is organized into six sections. In Section 1, the introduction to literature and key contributions are given. Section 2 contains the problem formulation. Sections 3 present the design of our algorithm ANN-SOS. Section 4 elaborates on the performance indicators used to validate our results. Section 5 is about results and discussion. In this section, we have presented the six sub-problems, detailed series solutions, unknown design weights obtained by ANN-SOS, graphical illustrations based on performance indicators, statistical analysis in terms of mean, best, and standard deviation for 100 independent simulations. Frequency histograms with normal distributions are given to support our claims. Section 6 concludes this research with future research topics.

II. PROBLEM FORMULATION

Heat exchangers play a vital role in heat dissipation from a hot surface. Rectangular fins are useful in many engineering designs. Rectangular fins are designed to cover the surface convection and radiation phenomena during heat transfer from primary hot surfaces. In this paper, we have analyzed the longitudinal fin models with three shapes rectangular, concave parabolic, and trapezoidal.

To present a mathematical model for this analysis, different symbols are used as follows:

- Length of a straight fin is denoted by L .
- T_b shows heat drawn by fin from base surface and T_a is the heat transfer by convection to the surrounding, T_s is heat radiation to an efficient sink attached with fins.
- k is the thermal conductivity of longitudinal fin.
- h and ϵ are convection heat transfer coefficient and emissivity of fin’s surface, respectively.

h and ϵ are temperature dependent and represented as in Equations (1), (2) and (3).

$$k = k_a[1 + \alpha(T - T_a)], \tag{1}$$

$$h = h_b \left[\frac{T - T_a}{T_b - T_a} \right]^m, \tag{2}$$

$$\epsilon = \epsilon_s[1 + \beta(T - T_s)], \tag{3}$$

where k_a represents the conduction of heat at temperature T_a . $(T_b - T_a)$ is the difference in temperatures and h_b is the convection heat transfer coefficient. ϵ_s is the emissivity at fin’s surface with temperature T_s . The variation in thermal conductivity and emissivity on the surface of fin are scaled by α and β , respectively.

As we are analyzing the longitudinal fins, thus with one-dimensional heat conduction, we can represent the energy equilibrium for straight fins as in Equation (4) [38]:

$$k_a \frac{d}{dx} \left[[1 + \alpha(T - T_a)]t(x) \frac{dT}{dx} \right] - h_b \left[\frac{T - T_a}{T_b - T_a} \right]^m (T - T_a) - \sigma \epsilon_s [1 + \beta(T - T_s)](T^4 - T_s^4) = 0, \tag{4}$$

where $t(x) = t_b + \delta((x/L)^n - 1)$, which is local semi-fin thickness. The values of n for rectangular, trapezoidal and concave parabolic profiles are 0, 1 and 2 respectively. The quantities t_b and δ define the semi-base thickness and fin taper respectively, see FIGURE 2. The boundary conditions for the problem are given as:

$$T(L) = T_b, \tag{5}$$

$$T'(0) = 0, \tag{6}$$

where T_b is the constant base temperature. Assuming the dimensionless parameters as follows:

$$\theta = \frac{T}{T_b}, \quad \theta_a = \frac{T_a}{T_b}, \quad \theta_s = \frac{T_s}{T_b}, \quad X = \frac{x}{L}, \quad C = \frac{\delta}{t_b},$$

$$N_c = \frac{h_b L^2 T_b^m}{k_a t_b (T_b - T_a)^m}, \quad A = \alpha T_b, \quad B = \beta T_b,$$

$$N_r = \frac{\sigma \epsilon_s L^2 T_b^3}{k_a t_b}, \quad \psi = \frac{t_b}{L}. \tag{7}$$

Therefore, using the dimensionless parameters the ODE for the problem of three profiles takes the form [38]:

$$\frac{d}{dX} \left[[1 + A(\theta - \theta_a)][1 + C(X^n - 1)] \frac{d\theta}{dX} \right] - N_c (\theta - \theta_a)^{m+1} - N_r [1 + B(\theta - \theta_s)](\theta^4 - \theta_s^4) = 0, \tag{8}$$

TABLE 1. Notations and abbreviations used in this paper.

Notation, Abbreviation	Description
NNs	Neural networks
ANNs	Artificial neural networks
MBB	Method of bilaterally bounded
ADM	Adomian decomposition method
HPM	Homotopy perturbation method
DTM	Differential transform method
PSO	Particle swarm optimization
DPSO	Darwinian particle swarm optimization
CS	Cuckoo search
SOS	Symbiotic organism search
RMSE	Root-mean-square error
AE	Absolute error
GD	Generational distance
MAD	Mean absolute deviation
NSE	Nash–Sutcliffe efficiency
ENSE	Error in Nash–Sutcliffe efficiency
PV	Parasite vector
MV	Mutual vector
L	Length
T_b	Temperature at base
T_a	Temperature at surrounding
T_s	Temperature at sink
k	Thermal conductivity
h	Heat transfer coefficient
ε	Fin’s surface emissivity
t_b	semi-base thickness
A	Thermal conductivity parameter
B	Emissivity parameter
N_c	Convection-conduction parameter
N_r	Radiation-conduction parameter
θ_a	Ratio of temperatures T_a to T_b
θ_s	Ratio of temperatures T_s to T_b
C	Fin taper ratio
ε_s	Emissivity with temperature T_s

and the boundary conditions are given as:

$$\theta(1) = 1, \quad \theta'(0) = 0. \tag{9}$$

Equation (8) shows that the thermal properties such as temperature distribution, heat transfer rate, efficiency and effectiveness of longitudinal fins depend on eight parameters that are thermal conductivity parameter (A), emissivity parameter (B), convection-conduction parameter (N_c), the

exponent (m) associated with convective heat transfer coefficient, radiation-conduction parameter (N_r), θ_a which is the ratio of temperature at surrounding (T_a) to temperature at base (T_b), θ_s is ratio of temperature at sink (T_s) to temperature at base (T_b) and fin taper ratio (C).

A. REFERENCE SOLUTIONS

For validation of our results and the ANN-SOS algorithm, we have used standard reference solutions, we have considered a simple case with the values of the following parameters $N_r = 0$, $A = 0$ and $m = 0$ used in Equation (8). The exact analytical solutions for the three profiles are given as [38]: For rectangular profile:

$$\theta(X) = C_1 e^{\sqrt{N_c}X} + C_2 e^{-\sqrt{N_c}X} + \theta_a, \tag{10}$$

For trapezoidal profile:

$$\theta(X) = C_1 J_0 \left(2\sqrt{-Nc} \left(\frac{1 + C(X - 1)}{C^2} \right) \right) + C_2 Y_0 \times \left(2\sqrt{-Nc} \left(\frac{1 + C(X - 1)}{C^2} \right) \right) + \theta_a, \tag{11}$$

For concave parabolic profile:

$$\theta(X) = C_1 P \left(\frac{\frac{1}{2} \frac{\sqrt{C+4W}-\sqrt{C}}{\sqrt{C}}}{\sqrt{C(C-1)}} \right) + C_2 Q \left(\frac{\frac{1}{2} \frac{\sqrt{C+4W}-\sqrt{C}}{\sqrt{C}}}{\sqrt{C(C-1)}} \right) + \theta_a, \tag{12}$$

where J_0 and Y_0 denote the 0^{th} -order Bessel functions of the first and second kind, respectively. In Equation (12), C_1 and C_2 are the constants that can be calculated using the boundary conditions. P and Q are Legendre polynomials of the first and second kind, respectively.

III. THE ANN-SOS APPROACH

In our paper, we have considered a real-life problem. The mathematical model of longitudinal heat transfer fins is derived and solved. An ANN-based series solution has been developed with log-sigmoid as activation function, see FIGURE 3, and the training of unknown weights in ANNs is performed by the Symbiotic Organism Search (SOS) algorithm. We name this approach as the ANN-SOS algorithm.

A. CONSTRUCTION OF ANN MODEL

A generalized approximate solution for the problem considered in this research and its nth derivative is given as [39]:

$$\hat{\theta}(X) = \sum_{i=1}^j \alpha_i f(\omega_i X + \beta_i), \tag{13}$$

$$\frac{d^n}{dX^n} \hat{\theta}(X) = \sum_{i=1}^j \alpha_i \frac{d^n}{dX^n} f(\omega_i X + \beta_i), \tag{14}$$

here α_i , β_i and ω_i are weights of ANN that are real and bounded, f represents the activation function, and j represents

the number of neurons in ANN. The log-sigmoid function has been used as activation function for ANN which is given as:

$$f(z) = \frac{1}{1 + e^{-z}}. \tag{15}$$

For the proposed neural model, the approximate solution and its second derivative is given by:

$$\hat{\theta}(X) = \sum_{i=1}^j \alpha_i \left(\frac{1}{1 + e^{-(\omega_i X + \beta_i)}} \right), \tag{16}$$

$$\hat{\theta}'(X) = \sum_{i=1}^j \alpha_i \omega_i \left(\frac{e^{-(\omega_i X + \beta_i)}}{(1 + e^{-(\omega_i X + \beta_i)})^2} \right), \tag{17}$$

$$\hat{\theta}''(X) = \sum_{i=1}^j \alpha_i \omega_i^2 \left(\frac{2e^{-2(\omega_i X + \beta_i)}}{(1 + e^{-(\omega_i X + \beta_i)})^3} - \frac{e^{-(\omega_i X + \beta_i)}}{(1 + e^{-(\omega_i X + \beta_i)})^2} \right). \tag{18}$$

B. OBJECTIVE FUNCTION

The sum of mean squared errors E_1 and E_2 is defined as the objective function which is given as:

$$\text{minimize } E = E_1 + E_2, \tag{19}$$

where E_1 is associated to ODE in the problem and E_2 is associated to initial or boundary conditions. For the problem of longitudinal fin heat transfer, E_1 and E_2 are given as:

$$E_1 = \frac{1}{N + 1} \sum_{m=0}^N \left(\frac{d}{dX} \left[[1 + A(\hat{\theta}_m - \theta_a)] [1 + C(X^n - 1)] \hat{\theta}'_m \right] - N_c(\hat{\theta} - \theta_a)^{m+1} - N_r [1 + B(\hat{\theta} - \theta_s)] (\hat{\theta}^4 - \theta_s^4) \right)^2, \tag{20}$$

$$E_2 = \frac{1}{2} ((\theta_1(X) - 1)^2 + (\theta'_0(X))^2). \tag{21}$$

In Equations (16,17,18), weights α , ω and β are adjustable parameters that are adjusted such that E_1 and E_2 approach to zero, then E also approaches zero. Hence, the given solution $\hat{\theta}(X)$ of the problem will represent the near exact solution $\theta(X)$.

C. THE SOS OPTIMIZER

The Symbiotic Organism Search (SOS) algorithm is used for training the neural networks to obtain the best weights. The SOS algorithm was first presented in [56]. SOS algorithm is inspired by different mutual relationships among organisms for their survival in the ecosystem. Based on different relationships, three phases of the algorithm are simulated; mutualism, commensalism, and parasitism. The characteristics of these relationships define the main principles of every phase. Relationships are beneficial for both of the organisms in mutualism phase; beneficial for one organism while

the other organism remains unaffected in the commensalism phase; useful for one organism and other organism is actively harmed in parasitism phase. Each organism randomly interacts with the other organisms throughout the three phases of SOS. The process is stopped if it meets the termination criterion; otherwise, it is repeated.

1) MUTUALISM PHASE

In the mutualism phase, two organisms have relationships with each other that give benefit to both of them. An example of mutualism is the relationship between honey bee and flowers, which is beneficial for both. Let X_i is i_{th} member of the ecosystem. It selects X_j randomly from the ecosystem for interaction. Each organism needs to improve its survival in the ecosystem, so it engages itself in a mutual relationship with other organisms. Based on their mutual symbiosis, the new candidate solutions are computed according to the equation:

$$X_{i\text{new}} = X_i + \text{rand}(0, 1) * (X_{\text{best}} - MV * BF_1), \tag{22}$$

$$X_{j\text{new}} = X_j + \text{rand}(0, 1) * (X_{\text{best}} - MV * BF_2), \tag{23}$$

$$MV = \frac{X_i + X_j}{2}, \tag{24}$$

$\text{rand}(0, 1)$ is a vector generated from random real numbers between 0 and 1. Here, the benefit factors BF_1 and BF_2 are defined randomly as it takes the value of either 1 or 2. These factors show up if an organism obtains benefit fully or partially. In Equation (24), mutual vector MV shows the characteristics of the relationship between organisms. In Equations (22,23), X_{best} shows the best degree of adaptation that increases the fitness of both of the organisms. Finally, if the new fitness value is better than the previous fitness, then it updates the organisms.

2) COMMENSALISM PHASE

The relationship between sharks and remora fish is an example of commensalism. The remora attaches itself to the shark's body and eats the leftover foods. Thus it obtains benefit. The activities of remora fish do not affect the shark, and thus the shark receives minimum benefit from the relationship if there is any. Just like the mutualism phase, the organism X_j is selected randomly from the ecosystem for interaction with other organisms X_i . At this stage, organism X_i obtains the benefit from the relationship with X_j . However, the organism X_j neither gets benefit nor affected by the interaction. Based on relationships between the organisms X_i and X_j , the alternative candidate solution for X_i is computed according to the Equation(25). Following these rules, the organism X_i is modified if its current fitness value is better than its previous value.

$$X_{i\text{new}} = X_i + \text{rand}(-1, 1) * (X_{\text{best}} - X_j), \tag{25}$$

The part of the equation, $(X_{\text{best}} - X_j)$, represents the benefit given by X_j to X_i increasing its survival in the ecosystem.

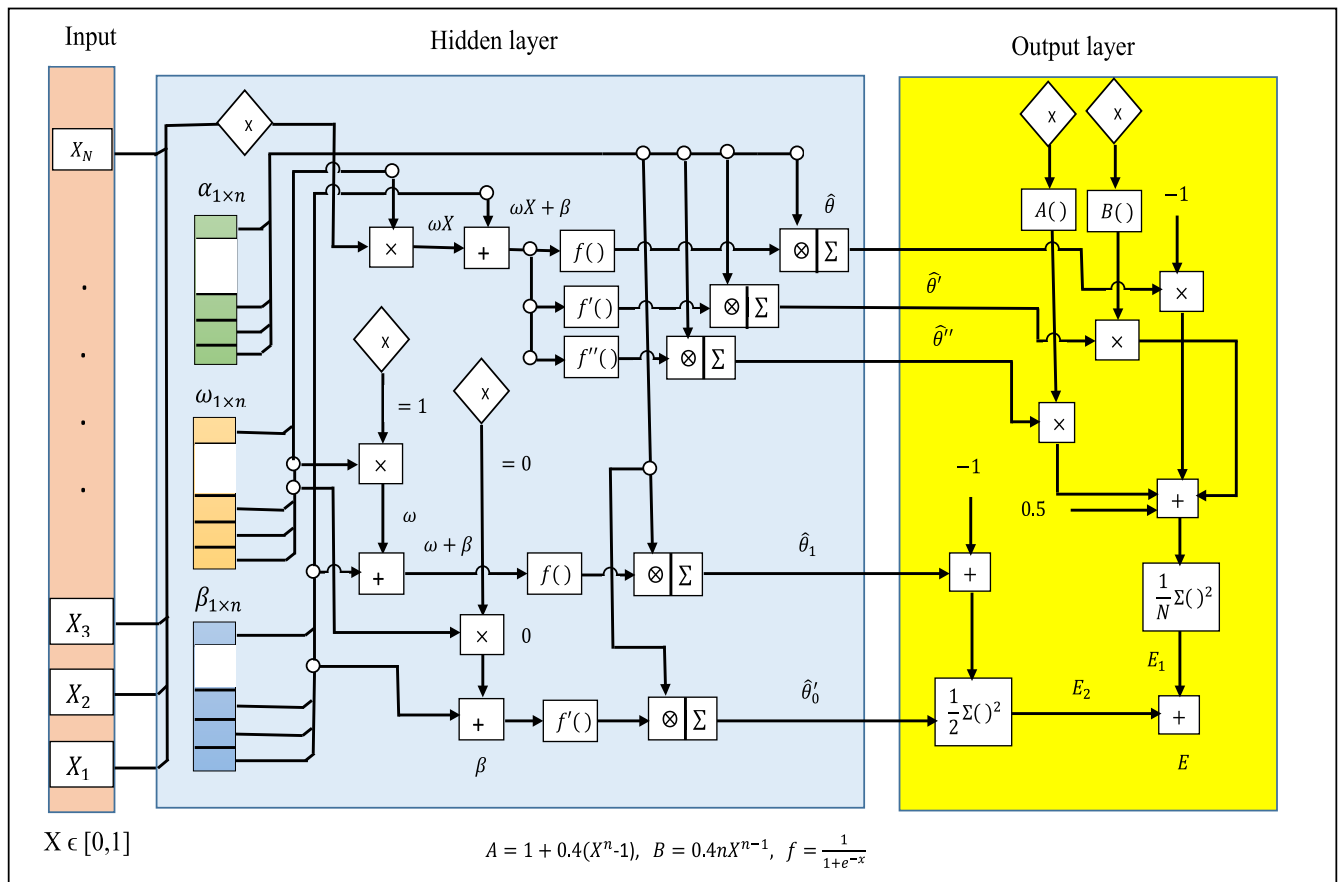


FIGURE 3. Illustration of artificial neural network architecture used in ANN-SOS procedure.

3) PARASITISM PHASE

Plasmodium parasite is the example of parasitism that uses the interaction with the anopheles mosquito and enters human hosts through it. When the parasite enters and reproduces itself inside the body of a human, the human affected by malaria, and as a result, he may die. In SOS, the organism X_i is selected as anopheles mosquito during the production of the artificial parasite known as “Parasite Vector” (PV). The PV is generated by duplicating the organism X_i in the solution space, then the dimensions which are selected randomly are modified by the use of a random number. The organism X_j is randomly chosen from the ecosystem and is given a job to host the parasite. The parasite attempts to adjust itself in place of X_j in the ecosystem. It tests both the members of the ecosystem for the estimation of their fitness values. If the parasite has the best fitness value in the ecosystem, it will harm the organism X_j and improves its position in the ecosystem. If the organism X_j has better fitness value, it will protect itself from the parasite, and the parasite will never have the option to live in the environment.

IV. PERFORMANCE METRICS

To check the efficiency of the designed technique, four types of statistical operators GD, MAD, TIC, and ENSE, have been

TABLE 2. Solutions obtained for rectangular profile in Case 1.

X	[38]	ANN-SOS	Absolute error
0	0.8240271	0.8240221	5.0667E-06
0.1	0.8256486	0.8256441	4.4967E-06
0.2	0.8305293	0.8305258	3.4708E-06
0.3	0.8387180	0.8387153	2.7859E-06
0.4	0.8502968	0.8502944	2.4016E-06
0.5	0.8653814	0.8653797	1.7055E-06
0.6	0.8841229	0.8841224	5.3481E-07
0.7	0.9067088	0.9067094	5.5744E-07
0.8	0.9333652	0.9333662	1.0249E-06
0.9	0.9643589	0.9643601	1.2255E-06
1	1.0000000	1.0000021	2.0742E-06

utilized. The mathematical formulation of the operators is given as:

$$GD = \frac{1}{n} \left(\sum_{i=1}^n (\theta_i - \hat{\theta}_i)^2 \right)^{1/2}, \tag{26}$$

$$MAD = \frac{1}{n} \sum_{i=1}^n |\theta_i - \hat{\theta}_i|, \tag{27}$$

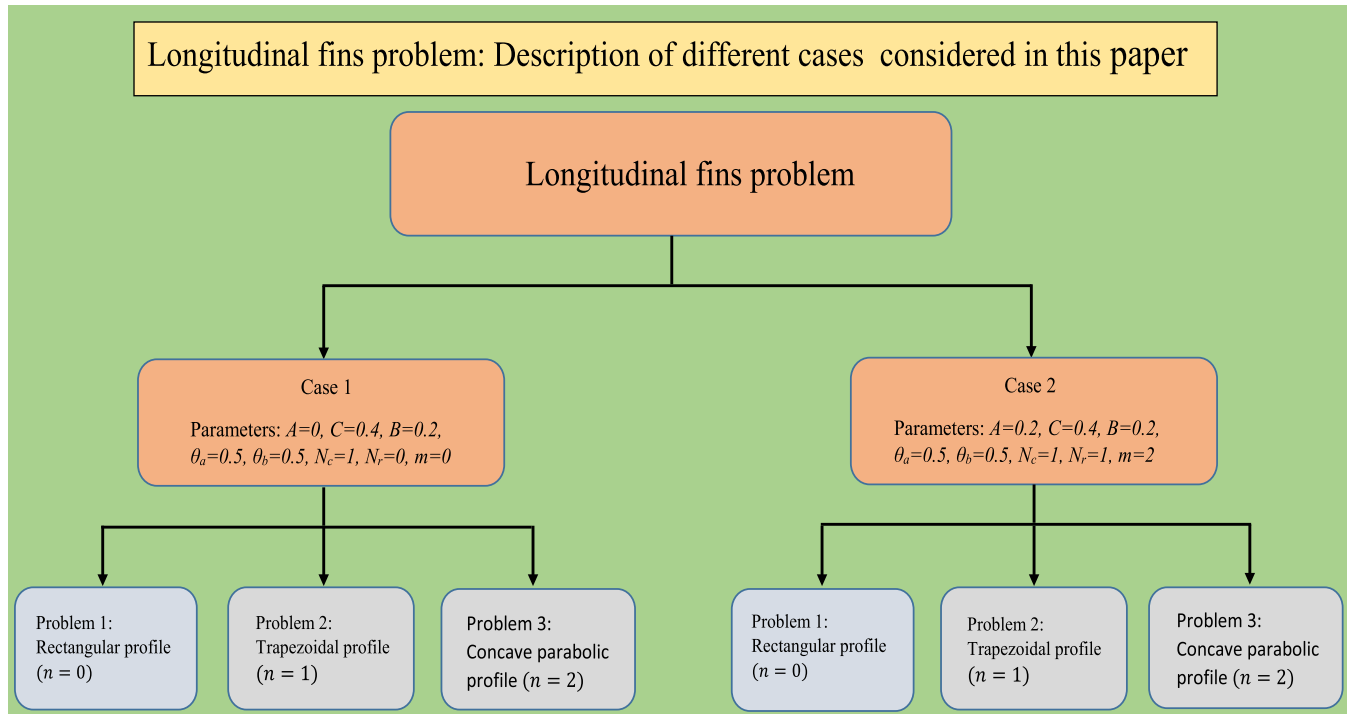


FIGURE 4. An overview of all problems analysed in this research.

TABLE 3. Solutions obtained for trapezoidal profile in Case 1.

X	[38]	ANN-SOS	Absolute error
0	0.80325	0.80337	1.1820E-04
0.1	0.80596	0.80580	1.6149E-04
0.2	0.81266	0.81273	5.8553E-05
0.3	0.82346	0.82375	2.7345E-04
0.4	0.83845	0.83855	7.4666E-05
0.5	0.85692	0.85693	2.2638E-05
0.6	0.87862	0.87876	1.1528E-04
0.7	0.90425	0.90397	2.8911E-04
0.8	0.93290	0.93255	3.4149E-04
0.9	0.96447	0.96454	6.3557E-05
1	1.00000	0.99997	4.0942E-05

TABLE 4. Solutions obtained for concave parabolic profile in Case 1.

X	[38]	ANN-SOS	Absolute error
0	0.79178	0.79163	1.5098E-04
0.1	0.79474	0.79405	6.8659E-04
0.2	0.80165	0.80127	3.7018E-04
0.3	0.81349	0.81313	3.5218E-04
0.4	0.82928	0.82938	1.0300E-04
0.5	0.84901	0.84969	6.8192E-04
0.6	0.87368	0.87373	5.0277E-05
0.7	0.90132	0.90113	1.8100E-04
0.8	0.93191	0.93154	3.6809E-04
0.9	0.96447	0.96461	1.3738E-04
1	1.00000	1.00004	4.1006E-05

$$TIC = \frac{\sqrt{\frac{1}{n} \sum_{i=1}^n (\theta_i - \hat{\theta}_i)^2}}{\left(\sqrt{\frac{1}{n} \sum_{i=1}^n \theta_i^2} + \sqrt{\frac{1}{n} \sum_{i=1}^n \hat{\theta}_i^2} \right)}, \quad (28)$$

$$NSE = 1 - \frac{\sum_{i=1}^n (\theta_i - \hat{\theta}_i)^2}{\sum_{i=1}^n (\theta_i - \bar{\theta}_i)^2}, \quad \bar{\theta}_i = \frac{1}{n} \sum_{i=1}^n \theta_i, \quad (29)$$

$$ENSE = 1 - NSE. \quad (30)$$

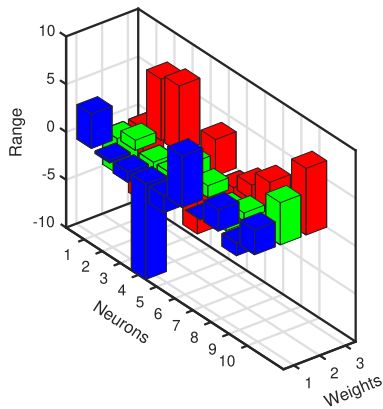
where n is the number of points in the approximate solution.

V. RESULTS AND DISCUSSION

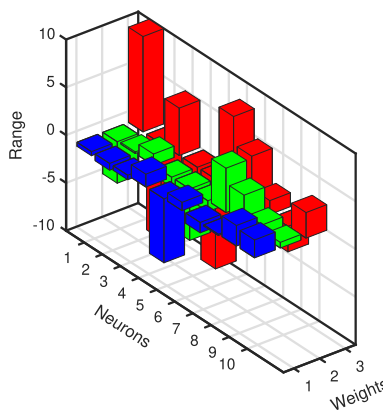
In this paper, the ANN-SOS algorithm is applied to solve the problem of heat transfer in distinct shapes of longitudinal heat

exchangers (fins). It is noted from Equation (8) that thermal properties, like temperature distribution in heat fins depend on thermal conductivity $A = \alpha T_b$, convection-conduction parameter $N_c = \frac{h_b L^2 T_b^m}{k_a t_b (T_b - T_a)^m}$, the exponent associated with convective heat transfer coefficient (m), radiation conduction parameter $N_r = \frac{\sigma \epsilon_s L^2 T_b^3}{k_a t_b}$.

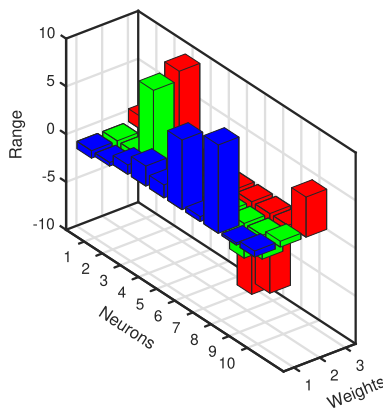
We have considered two cases of longitudinal fin designs with three profiles, such as rectangular, trapezoidal, and concave parabolic. The particularity of each case is different values of dimensionless quantities. We have divided our problem into two main scenarios and six sub-problems. Case 1 and 2 are different in terms of thermal conductivity parameter ($A = 0$, and 0.2), convective conduction parameter



(a) Weights for n=0.



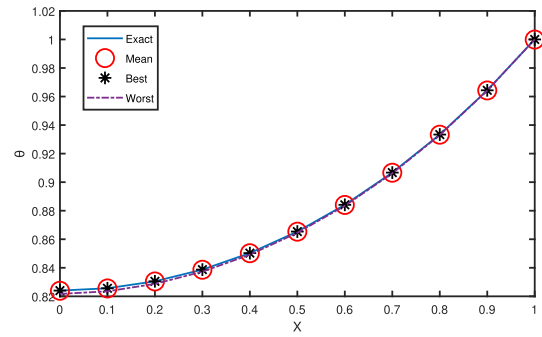
(b) Weights for n=1.



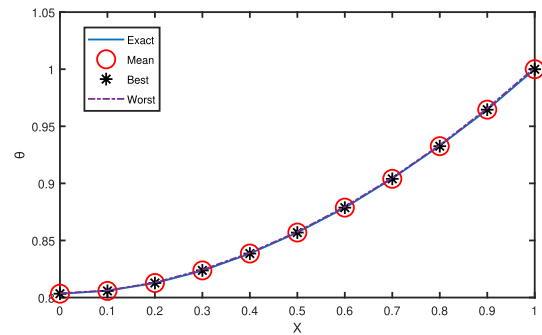
(c) Weights for n=2.

FIGURE 5. Weights obtained by ANN-SOS approach for Case 1.

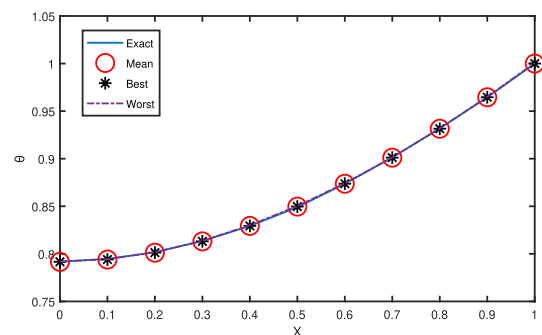
($N_c = 0$, and 0), exponent of convective heat transfer ($m = 0$, and 2), and radiation-conduction parameter ($N_r = 0$, and 1), respectively. In sub-problems for each case, we are considering three different designs (rectangular, trapezoidal, and concave parabolic) for $n = 0, 1, 2$ respectively, see FIGURES (2, and 4). For ANN architecture, each hidden layer is a sum of 10 neurons, and thus the number of unknown weights is 30. It varies the input variable in the interval $[0, 1]$ with a step size of $h = 1/10$, i.e., the entire domain contains



(a) Solutions for n=0.



(b) Solutions for n=1.



(c) Solutions for n=2.

FIGURE 6. Solutions obtained by ANN-SOS approach for Case 1.

11 grid points. We have simulated 100 runs of the ANN-SOS algorithm to get a better understanding of our novel approach.

A. CASE 1

In first case we have taken $A = 0$, $C = 0.4$, $B = 0.2$, $\theta_a = 0.5$, $\theta_s = 0.5$, $N_c = 1$, $N_r = 0$, and $m = 0$ so Equation (8) becomes as given below:

For rectangular profile ($n = 0$):

$$\begin{cases} \theta'' - \theta + 0.5 = 0, \\ \theta(1) = 1, \quad \theta'(0) = 0. \end{cases} \quad (31)$$

The objective function of Equation (31) is given as:

$$\min E = \frac{1}{11} \sum_{m=0}^N \left(\hat{\theta}_m'' - \hat{\theta}_m + 0.5 \right)^2 + \frac{1}{2} \left((\hat{\theta}_1 - 1)^2 + \hat{\theta}_0^2 \right). \quad (32)$$

TABLE 5. Absolute errors in solutions for Case 1.

X	Rectangular			Trapezoidal			Concave parabolic		
	Min	Mean	SD	Min	Mean	SD	Min	Mean	SD
0	1.48E-06	2.42E-04	3.91E-04	5.14E-06	2.01E-04	1.72E-04	2.65E-06	2.94E-04	2.13E-04
0.1	1.68E-07	2.25E-04	3.62E-04	3.06E-08	2.01E-04	1.87E-04	1.95E-05	7.59E-04	2.63E-04
0.2	2.65E-06	2.05E-04	3.26E-04	8.71E-06	1.61E-04	1.54E-04	6.12E-06	4.41E-04	2.09E-04
0.3	1.68E-07	1.83E-04	2.87E-04	1.03E-05	3.11E-04	1.71E-04	4.55E-06	4.02E-04	1.80E-04
0.4	9.09E-07	1.64E-04	2.53E-04	1.09E-06	1.61E-04	1.42E-04	4.72E-06	1.50E-04	1.45E-04
0.5	6.98E-07	1.50E-04	2.29E-04	1.46E-06	1.18E-04	1.44E-04	1.24E-04	6.58E-04	1.79E-04
0.6	5.35E-07	1.41E-04	2.17E-04	1.67E-08	1.92E-04	1.43E-04	9.25E-07	1.13E-04	1.32E-04
0.7	5.57E-07	1.38E-04	2.10E-04	1.25E-05	2.91E-04	1.66E-04	5.57E-06	2.53E-04	1.55E-04
0.8	1.02E-06	1.38E-04	2.06E-04	4.04E-05	3.44E-04	1.76E-04	6.05E-05	4.31E-04	1.86E-04
0.9	4.18E-08	1.36E-04	2.01E-04	2.43E-06	1.81E-04	1.78E-04	1.02E-06	1.62E-04	1.51E-04
1	2.29E-07	1.40E-04	1.97E-04	4.36E-08	1.56E-04	1.98E-04	6.32E-07	1.47E-04	1.68E-04

TABLE 6. Values of fitness function, GD and MAD for Case 1.

Problem	Fitness			GD			MAD		
	Best	Mean	Worst	Best	Mean	Worst	Best	Mean	Worst
n=0	2.32E-09	3.32E-06	3.56E-05	8.22E-07	5.54E-05	5.00E-04	2.30E-06	1.69E-04	1.60E-03
n=1	3.54E-08	2.17E-06	2.43E-05	5.02E-05	7.42E-05	2.87E-04	1.30E-04	2.11E-04	9.05E-04
n=2	1.33E-08	4.44E-06	6.08E-05	8.71E-05	1.29E-04	2.57E-04	2.33E-04	3.46E-04	7.62E-04

TABLE 7. TIC and ENSE values for Case 1.

Problem	TIC			ENSE		
	Best	Mean	Worst	Best	Mean	Worst
n=0	7.14E-07	4.81E-05	4.35E-04	5.26E-09	8.87E-05	2.62E-03
n=1	4.41E-05	6.52E-05	2.52E-04	1.58E-05	5.55E-05	7.62E-04
n=2	7.70E-05	1.15E-04	2.27E-04	4.84E-05	1.16E-04	5.20E-04

TABLE 8. Convergence analysis for Case 1.

Fin type	Fitness ≤			GD ≤			MAD ≤			TIC ≤			ENSE ≤		
	E-04	E-05	E-06	E-04	E-05	E-06	E-04	E-05	E-06	E-04	E-05	E-06	E-04	E-05	E-06
Rectangular	100	91	47	100	85	22	97	58	5	100	87	27	97	85	58
Trapezoidal	100	100	98	100	89	0	100	0	0	100	92	0	100	93	0
Concave parabolic	100	100	92	100	4	0	100	0	0	100	34	0	100	63	0

For trapezoidal profile (n = 1):

$$\begin{cases} \theta'' + 0.4(X - 1)\theta'' + 0.4\theta' - \theta + 0.5 = 0, \\ \theta(1) = 1, \quad \theta'(0) = 0. \end{cases} \quad (33)$$

The objective function Equation (33) is given as:

$$\min E = \frac{1}{11} \sum_{m=0}^N \left(\hat{\theta}_m'' + 0.4(X - 1)\hat{\theta}_m'' + 0.4\hat{\theta}_m' - \hat{\theta}_m + 0.5 \right)^2 + \frac{1}{2} \left((\hat{\theta}_1 - 1)^2 + \hat{\theta}_0^2 \right). \quad (34)$$

For concave parabolic profile (n = 2):

$$\begin{cases} \theta'' + 0.4(X^2 - 1)\theta'' + 0.8X\theta' - \theta + 0.5 = 0, \\ \theta(1) = 1, \quad \theta'(0) = 0. \end{cases} \quad (35)$$

The objective function for Equation (35) is given as:

$$\min E = \frac{1}{11} \sum_{m=0}^N \left(\hat{\theta}_m'' + 0.4(X^2 - 1)\hat{\theta}_m'' + 0.8X\hat{\theta}_m' - \hat{\theta}_m + 0.5 \right)^2 + \frac{1}{2} \left((\hat{\theta}_1 - 1)^2 + \hat{\theta}_0^2 \right). \quad (36)$$

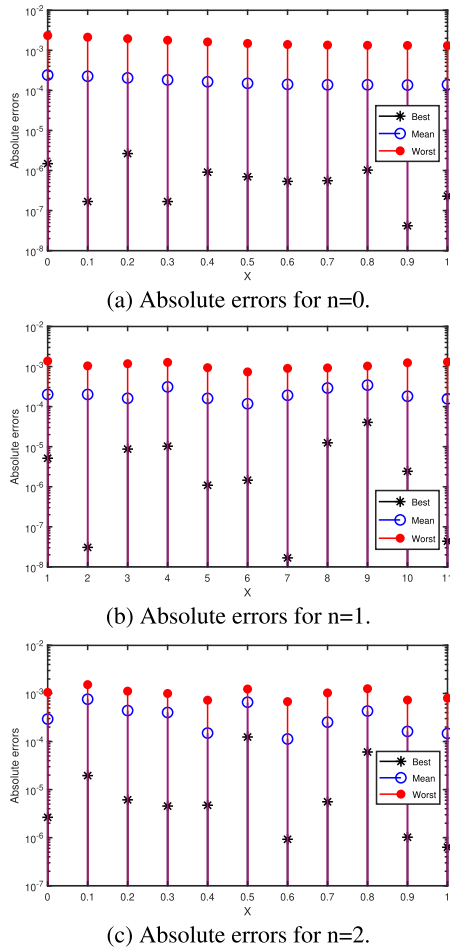


FIGURE 7. Absolute errors in solutions obtained for Case 1.

We have taken 10 number of neurons in our model. Solution obtained by ANN-SOS consists of 10 terms, each term corresponds to one neuron. The terms of the solution are in the form of sigmoid function. Series solutions obtained by the ANN-SOS algorithm for Case 1 are as follows:

Solution for rectangular profile (n = 0):

$$\hat{\theta}_{C1(n=0)} = \frac{3.61749042497874}{1 + e^{-(-3.67068627674519 * X - 7.62607165537628)}} - \frac{0.282320091002557}{1 + e^{-(-1.06021414289694 * X + 6.41220030130322)}} - \frac{1.08751429237298}{1 + e^{-(-1.60386107405839 * X + 6.93566998353666)}} + \frac{9.98717589716628}{1 + e^{-(-1.07531327107981 * X - 7.30215598226350)}} - \frac{1.77618317588448}{1 + e^{-(-2.30684663036297 * X + 3.80813738209909)}} + \frac{5.39818281068250}{1 + e^{-(-1.24366927544579 * X - 3.79745101946880)}} - \frac{0.0550131513142178}{1 + e^{-(-2.22731328201466 * X + 1.51207818967573)}}$$

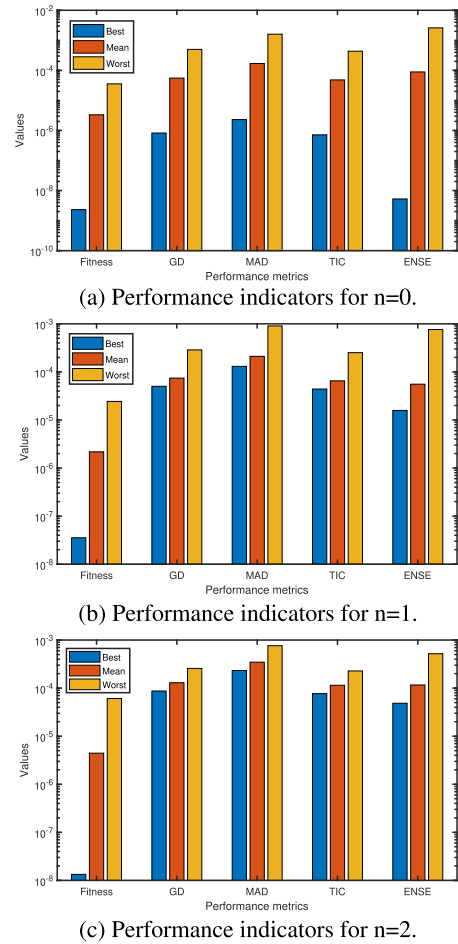
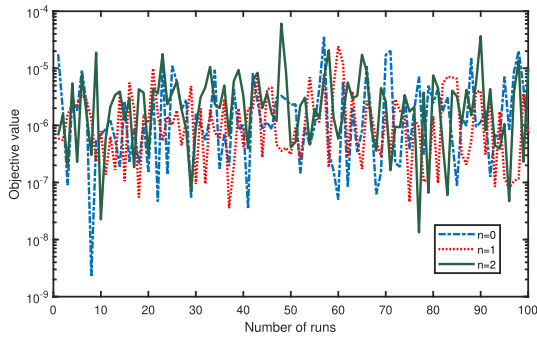


FIGURE 8. Performance indicators obtained for Case 1.

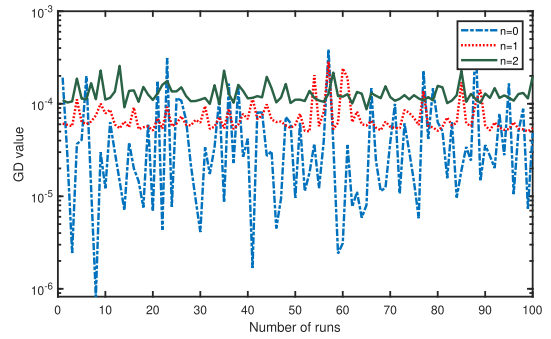
$$\begin{aligned} & + \frac{2.22691407108311}{1 + e^{-(0.872094818432651 * X + 3.03599758882442)}} \\ & - \frac{1.34064466035852}{1 + e^{-(0.572621713185842 * X + 0.650545769938320)}} \\ & + \frac{2.62018734698392}{1 + e^{-(4.41303712761091 * X + 6.96242270155723)}} \end{aligned} \quad (37)$$

Solution for trapezoidal profile (n = 1):

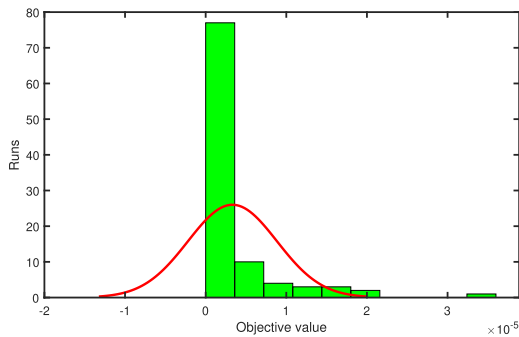
$$\hat{\theta}_{C1(n=1)} = \frac{-0.427629310120337}{1 + e^{-(-4.33907794991442 * X + 9.96797298362664)}} - \frac{0.709252021861192}{1 + e^{-(-0.171601966462608 * X - 9.99804382178738)}} - \frac{0.470418542676985}{1 + e^{-(-1.18038033702902 * X + 4.95180620081143)}} + \frac{1.34466446676355}{1 + e^{-(-1.02337967178866 * X - 2.27584213901628)}} - \frac{6.69029592738523}{1 + e^{-(-5.37695864049995 * X - 9.39513015380921)}} + \frac{0.868652143586056}{1 + e^{-(-1.13317686880999 * X + 7.77787715576440)}} - \frac{1.08413748379396}{1 + e^{-(-4.63966368881078 * X + 4.86278384038115)}}$$



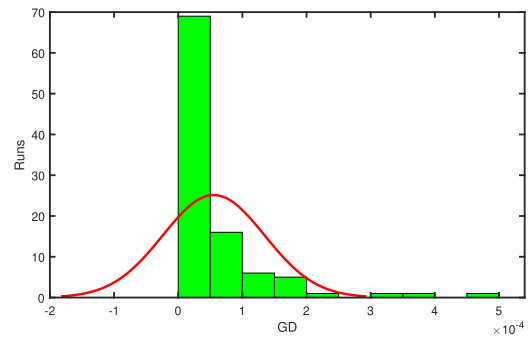
(a) Fitness values for case 1.



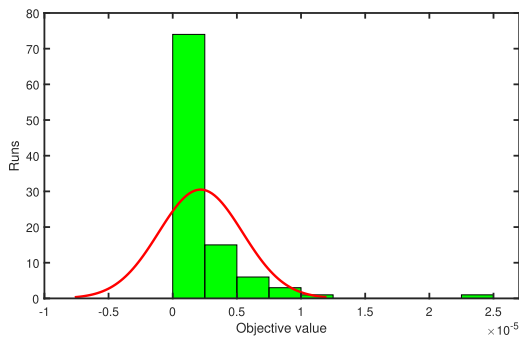
(a) GD values for case 1.



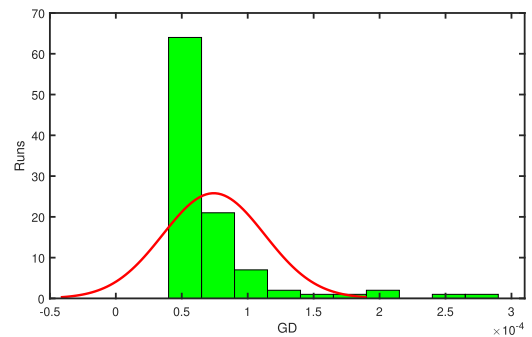
(b) Fitness values for n=0.



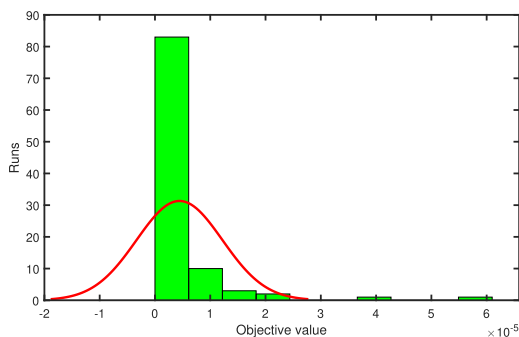
(b) GD values for n=0.



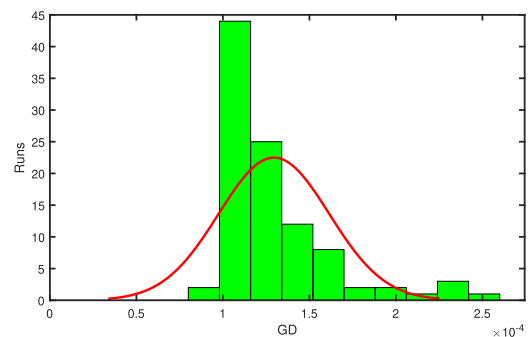
(c) Fitness values for n=1.



(c) GD values for n=1.



(d) Fitness values for n=2.



(d) GD values for n=2.

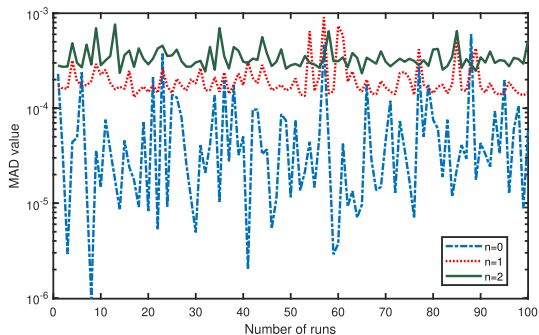
FIGURE 9. Results in terms of fitness values obtained for Case 1.

FIGURE 10. Results in terms of GD values obtained for Case 1.

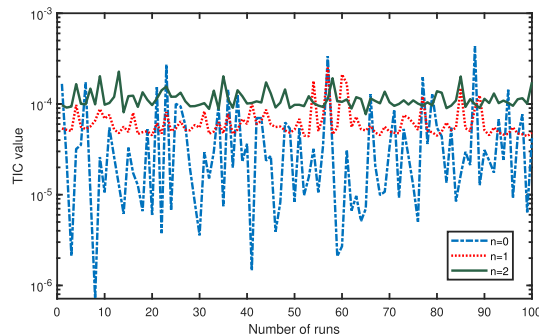
$$\begin{aligned}
 & \frac{-0.136863661097504}{1 + e^{-(3.05263995739417 * X + 1.45126098873239)}} \\
 & + \frac{2.15182460779979}{1 + e^{-(1.18037371768373 * X - 2.67380293002561)}} \\
 & + \frac{1.87403327686806}{1 + e^{-(0.588890522860738 * X + 2.67285441850872)}} \cdot (38)
 \end{aligned}$$

DISCUSSION ON RESULTS FOR CASE 1:

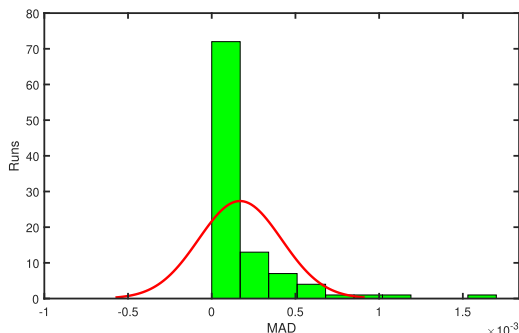
The objective values (mean squared errors (MSE)) obtained for rectangular, trapezoidal and concave parabolic profiles are $2.3154e - 09$, $3.5428e - 08$ and $1.3345e - 08$, respectively, see TABLE (4). The set of best weights for these



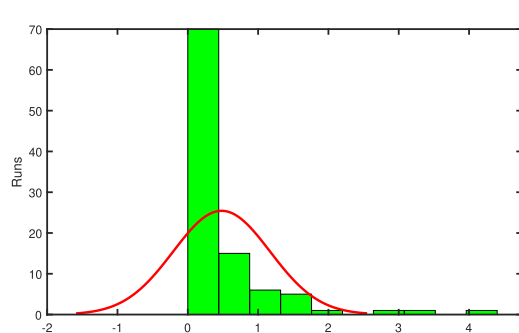
(a) MAD values for case 1.



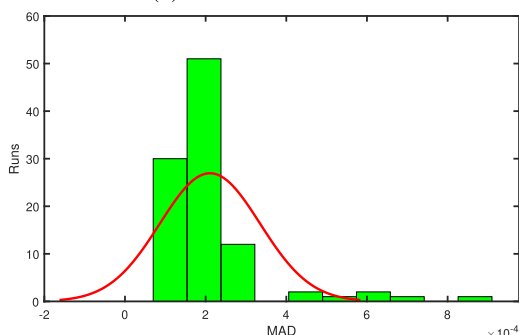
(a) TIC values for case 1.



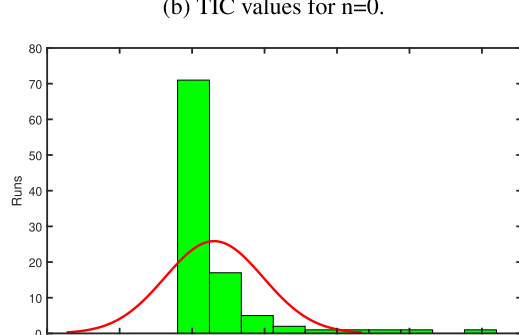
(b) MAD values for n=0.



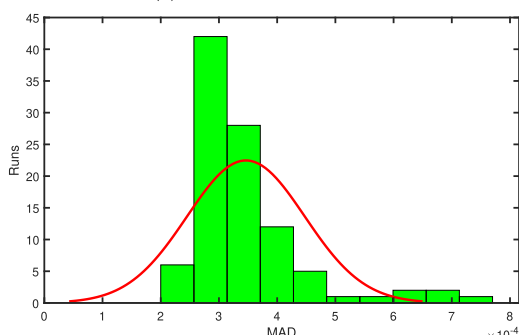
(b) TIC values for n=0.



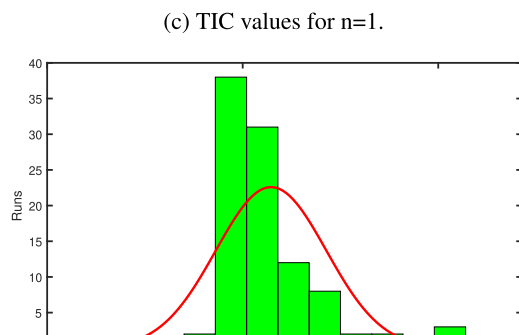
(c) MAD values for n=1.



(c) TIC values for n=1.



(d) MAD values for n=2.



(d) TIC values for n=2.

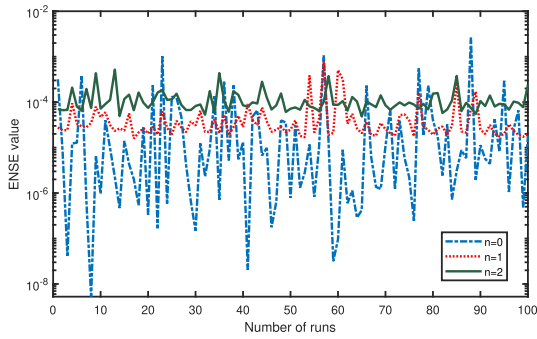
FIGURE 11. Results in terms of MAD values obtained for Case 1.

three profiles are presented in FIGURE (5). The approximate solutions for different profiles are given in TABLES (2,3,4) and FIGURE (6). **Solution for concave parabolic profile (n = 2):**

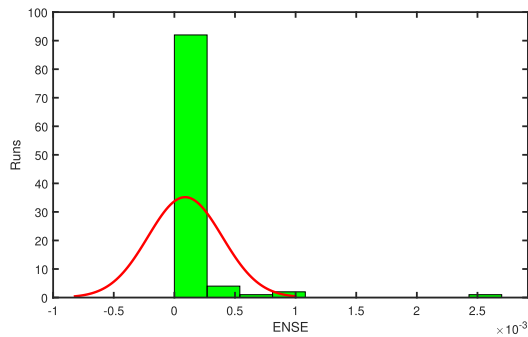
$$\hat{\theta}_{C1(n=2)}$$

FIGURE 12. Results in terms of TIC values obtained for Case 1.

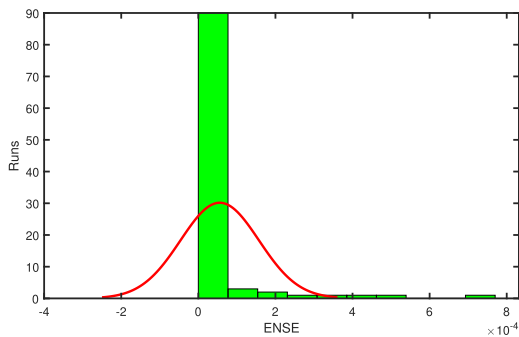
$$= \frac{-0.782218806733728}{1 + e^{-(-1.52180582504944 * X + 1.33831407213679)}} + \frac{-0.375457701967646}{1 + e^{-(-2.39227970367793 * X + 4.50436164112033)}}$$



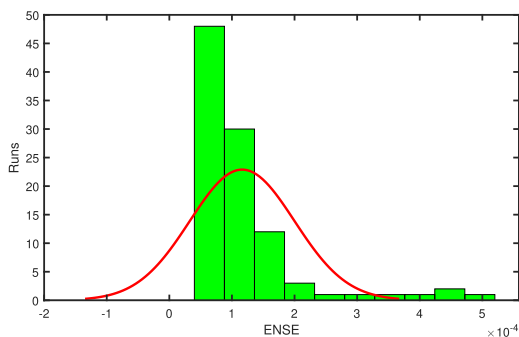
(a) ENSE values for case 1.



(b) ENSE values for n=0.



(c) ENSE values for n=1.



(d) ENSE values for n=2.

FIGURE 13. Results in terms of ENSE values obtained for Case 1.

$$\begin{aligned}
 & + \frac{0.982314559759026}{1 + e^{-(7.74974673860756 * X + 8.71464171226744)}} \\
 & + \frac{2.09901669877859}{1 + e^{-(1.55112625160013 * X - 3.71391281519073)}}
 \end{aligned}$$

TABLE 9. Solutions obtained for rectangular profile in Case 2.

X	[38]	ANN-SOS	Absolute error
0	0.78855	0.78871	1.5907E-04
0.1	0.79036	0.79044	8.0569E-05
0.2	0.79578	0.79569	9.5759E-05
0.3	0.80482	0.80456	2.5518E-04
0.4	0.81747	0.81726	2.1210E-04
0.5	0.83464	0.83405	5.9078E-04
0.6	0.85542	0.85534	8.4955E-05
0.7	0.88163	0.88168	5.4682E-05
0.8	0.91416	0.91383	3.2737E-04
0.9	0.95301	0.95278	2.2877E-04
1	1.00000	0.99991	8.6326E-05

$$\begin{aligned}
 & + \frac{1.35749577052221}{1 + e^{-(0.843736071584196 * X - 3.78041878064892)}} \\
 & + \frac{7.29978869415915}{1 + e^{-(0.419716218903707 * X - 5.15438599518447)}} \\
 & + \frac{0.516779652103827}{1 + e^{-(2.30457565425263 * X - 9.68700491798374)}} \\
 & + \frac{9.24750012608333}{1 + e^{-(3.63150107321958 * X - 8.33042229605450)}} \\
 & + \frac{0.240245621476915}{1 + e^{-(2.49994074514838 * X - 0.943308589743724)}} \\
 & + \frac{0.617920226517735}{1 + e^{-(0.612291243998232 * X + 4.19821187908109)}} \cdot (39)
 \end{aligned}$$

In FIGURE (6), the best, mean and worst of all solutions are plotted and it is clear from the FIGURE that all the solutions including the worst solution are very close to the exact solution which shows the efficiency of the ANN-SOS algorithm. The absolute errors in the solutions are given in TABLE (5) and also plotted in FIGURE (7). Absolute errors in the solutions for rectangular, trapezoidal and concave parabolic profiles range from 10^{-06} to 10^{-08} , 10^{-05} to 10^{-08} and 10^{-04} to 10^{-07} , respectively. The best, mean and worst values of fitness function and performance metrics are given in TABLES (6,7) and FIGURE (8). The values of performance metrics range from 10^{-03} to 10^{-09} . Convergence analysis for case 1 is given in TABLE (8). Histogram plots of fitness values with normal distribution fittings for different profiles are given in FIGURE (9). FIGURE (9) shows that more than 80% of fitness values are less than 10^{-05} . In FIGURES (10,11,12) and (13), we have plotted the histograms with normal distribution fittings for performance indicators GD, MAD, TIC and ENSE for rectangular, trapezoidal and concave parabolic profiles. It is evident from these FIGURES that more than 90% of the values of performance metrics are less than 10^{-03} , which shows the efficiency and accuracy in the results of the ANN-SOS algorithm. It is observed from TABLES (2-4) and FIGURE (6a, 6b, and 6c) that in case 1 temperature distribution ranges between 0.8240271

TABLE 10. Solutions obtained for trapezoidal profile in Case 2.

X	[38]	ANN-SOS	Absolute error
0	0.771386	0.771137	2.4853E-04
0.1	0.773193	0.773618	2.2485E-04
0.2	0.780422	0.780733	3.1089E-04
0.3	0.792169	0.792153	1.5937E-05
0.4	0.807530	0.807728	1.9785E-04
0.5	0.827410	0.827466	5.6416E-05
0.6	0.851807	0.851525	2.8252E-04
0.7	0.880723	0.880215	5.0805E-04
0.8	0.914157	0.914018	1.3824E-04
0.9	0.953916	0.953626	2.8999E-04
1	1.000000	0.999998	2.2907E-06

to 1 (for rectangular profile), 0.80325 to 1 (for trapezoidal profile), (0.79178 to 1) (for concave parabolic profile). Moreover, for a better understanding of frequency plots, we have presented TABLE 8. In this TABLE, we have given success rates of different thresholds for fitness values, GD, MAD, TIC, and ENSE. Our solutions and errors in solutions are compared with solutions calculated in [38], see TABLES (2-4). For each profile, the ANN-SOS algorithm is successful in getting solutions to better quality with minimum errors.

B. CASE 2

In second case, we have taken $A = 0.2, C = 0.4, B = 0.2, \theta_a = 0.5, \theta_b = 0.5, N_c = 1, N_r = 1$ and $m = 2$. Using these values Equation (8) becomes:

For rectangular profile (n = 0):

$$\begin{cases} \theta'' + 0.2((\theta - 0.5)\theta'' + \theta^2) - (\theta - 0.5)^3 - (0.9 + 0.2\theta) \\ (\theta^4 - 0.0625) = 0, \\ \theta(1) = 1, \quad \theta'(0) = 0. \end{cases} \quad (40)$$

The objective function for Equation (40) is given as:

$$\begin{aligned} E = \frac{1}{11} \sum_{m=0}^N & \left(\hat{\theta}_m'' + 0.2((\hat{\theta}_m - 0.5)\hat{\theta}_m'' + \hat{\theta}_m'^2) - (\hat{\theta}_m - 0.5)^3 \right. \\ & \left. - (0.9 + 0.2\hat{\theta}_m)(\hat{\theta}_m^4 - 0.0625) \right)^2 + \frac{1}{2} \left((\hat{\theta}_1 - 1)^2 \right. \\ & \left. + \hat{\theta}_0'^2 \right). \end{aligned} \quad (41)$$

For trapezoidal profile (n = 1):

$$\begin{cases} (0.54 + 0.36X + 0.12\theta + 0.08X\theta)\theta'' + \theta'(0.36 \\ + 0.12\theta' + 0.08(X\theta' + \theta)) - (\theta - 0.5)^3 - (0.9 \\ + 0.2\theta)(\theta^4 - 0.0625) = 0, \\ \theta(1) = 1, \quad \theta'(0) = 0. \end{cases} \quad (42)$$

TABLE 11. Solutions obtained for concave parabolic profile in Case 2.

X	[38]	ANN-SOS	Absolute error
0	0.761446	0.761706	2.6058E-04
0.1	0.764157	0.764130	2.6696E-05
0.2	0.771386	0.771391	5.0197E-06
0.3	0.783133	0.783430	2.9776E-04
0.4	0.800301	0.800165	1.3617E-04
0.5	0.821084	0.821526	4.4192E-04
0.6	0.847289	0.847494	2.0524E-04
0.7	0.878012	0.878120	1.0827E-04
0.8	0.913253	0.913549	2.9619E-04
0.9	0.954819	0.954057	7.6181E-04
1	1.000000	1.000094	9.4414E-05

TABLE 12. Values of TIC and ENSE for Case 2.

Problem	TIC			ENSE		
	Best	Mean	Worst	Best	Mean	Worst
n=0	5.59E-05	2.83E-04	2.71E-03	2.28E-05	2.24E-03	8.92E-02
n=1	6.59E-05	1.50E-04	7.63E-04	3.81E-05	3.47E-04	5.62E-03
n=2	8.25E-05	1.53E-04	6.82E-04	3.68E-05	2.74E-04	4.28E-03

The objective function for Equation (42) is given by:

$$\begin{aligned} E = \frac{1}{11} \sum_{m=0}^N & \left((0.54 + 0.36X + 0.12\hat{\theta}_m + 0.08X\hat{\theta}_m)\hat{\theta}_m'' \right. \\ & \left. + \hat{\theta}_m'(0.36 + 0.12\hat{\theta}_m' + 0.08(X\hat{\theta}_m' + \hat{\theta}_m)) - (\hat{\theta}_m \right. \\ & \left. - 0.5)^3 - (0.9 + 0.2\hat{\theta}_m)(\hat{\theta}_m^4 - 0.0625) \right)^2 \\ & \left. + \frac{1}{2} \left((\hat{\theta}_1 - 1)^2 + \hat{\theta}_0'^2 \right). \end{aligned} \quad (43)$$

For concave parabolic profile (n = 2):

$$\begin{cases} (0.54 + 0.36X^2 + 0.12\theta + 0.08X^2\theta)\theta'' + \theta'(0.72X \\ + 0.12\theta' + 0.08(X^2\theta' + 2X\theta)) - (\theta - 0.5)^3 \\ - (0.9 + 0.2\theta)(\theta^4 - 0.0625) = 0, \\ \theta(1) = 1, \quad \theta'(0) = 0. \end{cases} \quad (44)$$

The objective function for Equation (44) is given as:

$$\begin{aligned} E = \frac{1}{11} \sum_{m=0}^N & \left((0.54 + 0.36X^2 + 0.12\hat{\theta}_m + 0.08X^2\hat{\theta}_m)\hat{\theta}_m'' \right. \\ & \left. + \hat{\theta}_m'(0.72X + 0.12\hat{\theta}_m' + 0.08(X^2\hat{\theta}_m' + 2X\hat{\theta}_m)) \right. \\ & \left. - (\hat{\theta}_m - 0.5)^3 - (0.9 + 0.2\hat{\theta}_m)(\hat{\theta}_m^4 - 0.0625) \right)^2 \\ & \left. + \frac{1}{2} \left((\hat{\theta}_1 - 1)^2 + \hat{\theta}_0'^2 \right). \end{aligned} \quad (45)$$

TABLE 13. Absolute errors in solutions for Case 2.

X	Rectangular			Trapezoidal			Concave parabolic		
	Min	Mean	SD	Min	Mean	SD	Min	Mean	SD
0	6.81E-06	8.76E-04	1.54E-03	2.43E-05	5.41E-04	4.34E-04	6.41E-06	3.51E-04	3.02E-04
0.1	6.95E-06	8.28E-04	1.37E-03	5.55E-06	4.26E-04	3.43E-04	5.11E-06	3.45E-04	3.68E-04
0.2	4.60E-06	8.52E-04	1.23E-03	1.89E-05	3.61E-04	3.27E-04	1.79E-06	2.86E-04	3.30E-04
0.3	2.12E-05	9.09E-04	1.13E-03	1.30E-06	3.04E-04	3.65E-04	8.98E-06	3.10E-04	2.35E-04
0.4	5.61E-06	8.34E-04	1.07E-03	3.59E-06	3.07E-04	3.47E-04	1.04E-05	3.38E-04	3.29E-04
0.5	1.43E-05	1.14E-03	1.11E-03	2.21E-06	2.93E-04	3.92E-04	3.91E-06	4.15E-04	2.66E-04
0.6	1.17E-06	7.73E-04	1.14E-03	3.86E-06	4.98E-04	4.75E-04	2.07E-06	3.13E-04	3.70E-04
0.7	4.67E-07	7.98E-04	1.21E-03	4.75E-05	7.42E-04	5.67E-04	1.52E-07	3.60E-04	4.90E-04
0.8	4.10E-05	1.19E-03	1.39E-03	3.54E-06	5.12E-04	6.23E-04	1.80E-07	4.37E-04	5.05E-04
0.9	1.56E-05	1.21E-03	1.51E-03	7.81E-06	6.78E-04	7.13E-04	3.05E-06	1.19E-03	7.37E-04
1	5.84E-06	1.18E-03	1.67E-03	2.89E-08	5.68E-04	7.97E-04	6.91E-07	5.54E-04	7.21E-04

The mathematical forms of approximate solutions $\hat{\theta}$ for rectangular, trapezoidal and concave parabolic profiles are given Equations(46,47) and (48).

DISCUSSION ON RESULTS FOR CASE 2:

The objective values (absolute errors in solutions) obtained for rectangular, trapezoidal and concave parabolic profiles are

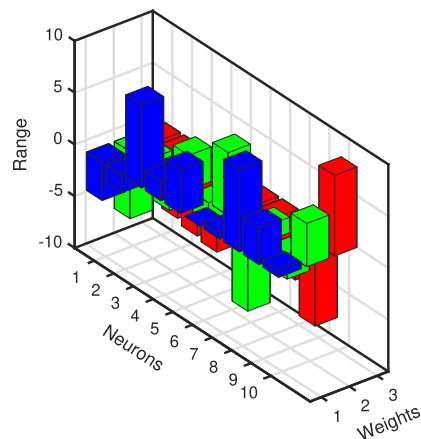
TABLE 14. Values of fitness function, GD and MAD for Case 2.

Problem	Fitness			GD			MAD		
	Best	Mean	Worst	Best	Mean	Worst	Best	Mean	Worst
n=0	3.58E-07	5.78E-05	5.19E-04	6.25E-05	3.16E-04	3.00E-03	1.58E-04	9.63E-04	9.87E-03
n=1	8.58E-09	1.69E-05	1.21E-04	7.29E-05	1.66E-04	8.43E-04	2.10E-04	4.76E-04	2.55E-03
n=2	1.41E-07	2.05E-05	1.29E-04	9.09E-05	1.69E-04	7.49E-04	2.11E-04	4.45E-04	2.27E-03

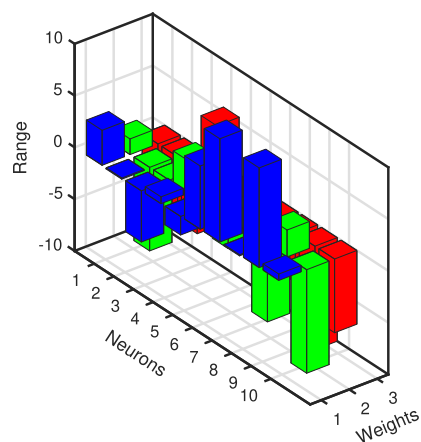
3.5775e – 07, 8.5797e – 09 and 1.4071e – 07, respectively. The best set of ANN weights are depicted in FIGURE (14). The numerical solutions obtained for all of the three profiles are given TABLES (9,10,11). The solutions for all the profiles

TABLE 15. Convergence analysis for case 2.

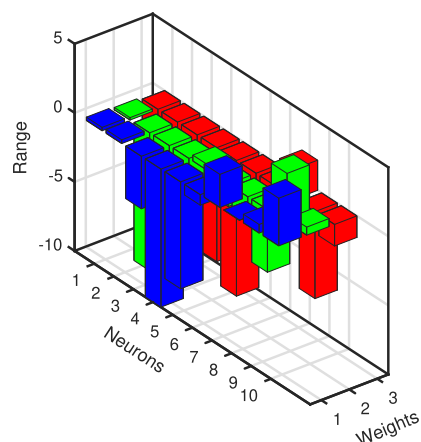
Fin type	Fitness \leq					GD \leq					MAD \leq					TIC \leq					ENSE \leq				
	E-03	E-04	E-05	E-03	E-04	E-05	E-03	E-04	E-05	E-03	E-04	E-05	E-03	E-04	E-05	E-03	E-04	E-05	E-03	E-04	E-05				
Rectangular	100	100	77	100	98	31	100	100	100	100	65	0	100	100	100	98	69	36	98	94	36				
Trapezoidal	100	100	99	100	100	45	100	100	100	94	0	100	100	100	100	100	94	47	100	50					
Concave parabolic	100	100	96	100	100	25	100	100	100	94	0	100	100	100	100	100	95	40	100	60					



(a) Weights for n=0.



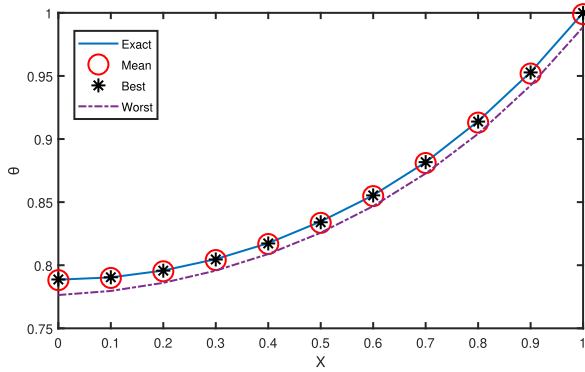
(b) Weights for n=1.



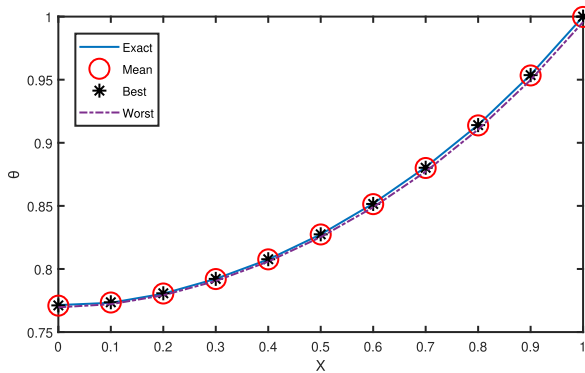
(c) Weights for n=2.

FIGURE 14. Weights obtained by ANN-SOS approach for Case 2.

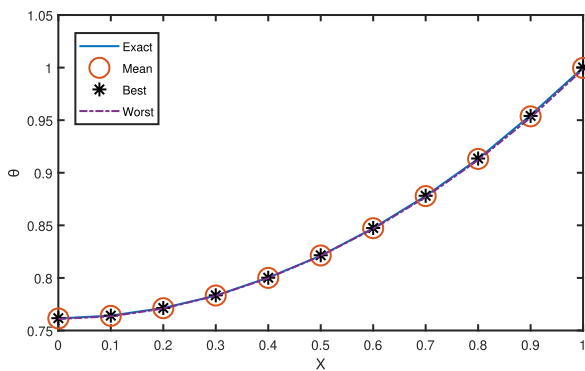
are compared with the exact solution in FIGURE (15), and we can see that the best and mean of all 100 solutions obtained by ANN-SOS algorithm for the problems are very close to the exact solution. In the case of trapezoidal and concave



(a) Solutions for n=0.



(b) Solutions for n=1.

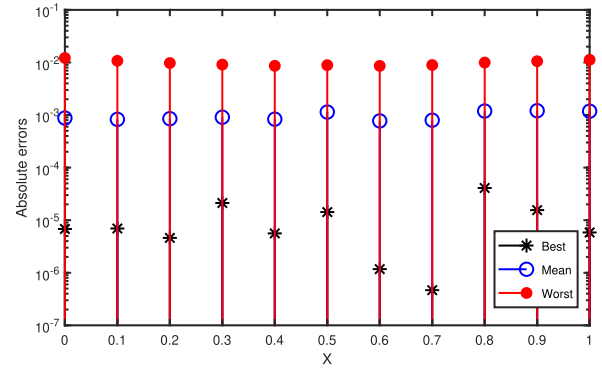


(c) Solutions for n=2.

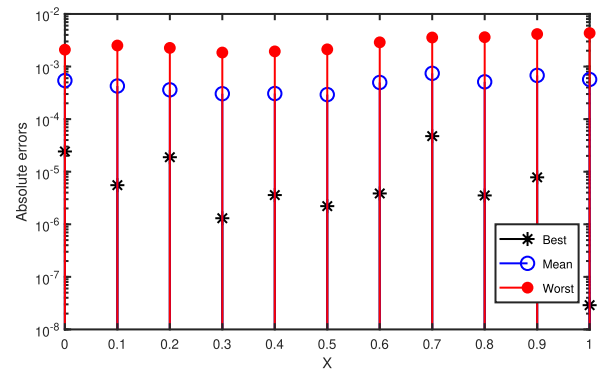
FIGURE 15. Solutions obtained by ANN-SOS approach for Case 2.

parabolic, the worst solutions are also very close to the exact solution, which shows the accuracy of the solutions obtained by the ANN-SOS algorithm. The absolute errors between the exact and approximate solutions are given in TABLE (13). For the problem of the rectangular profile, the absolute minimum errors in the solutions lie between 10^{-5} to 10^{-7} , and the mean values of the errors are between 10^{-3} to 10^{-4} .
Solution for rectangular profile (n = 0):

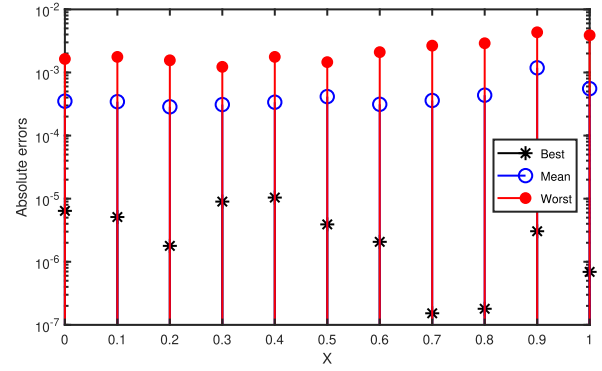
$$\begin{aligned} \hat{\theta}_{C2(n=0)} &= \frac{-3.69693215035094}{1 + e^{-(-6.47918949718765 * X - 5.76360774195530)}} \\ &+ \frac{-1.70284654099295}{1 + e^{-(-0.510164139745732 * X - 6.25466761712446)}} \end{aligned}$$



(a) Absolute errors for n=0.



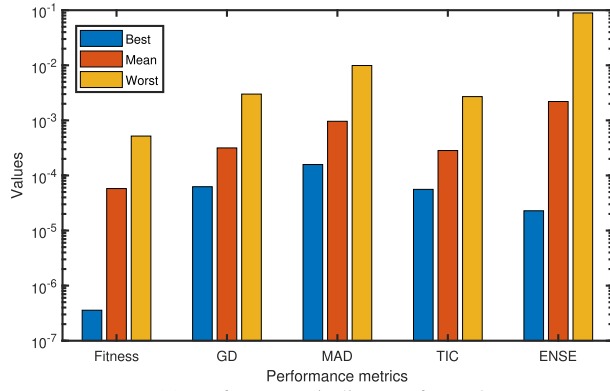
(b) Absolute errors for n=1.



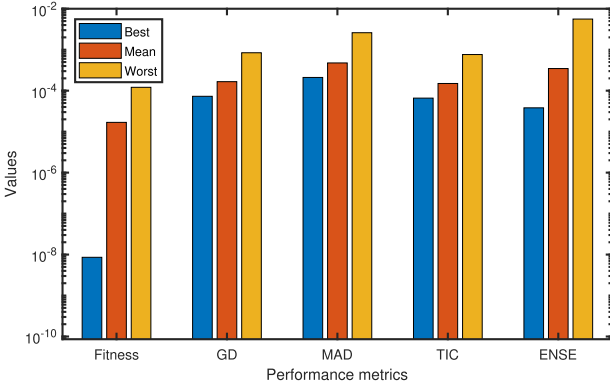
(c) Absolute errors for n=2.

FIGURE 16. Absolute errors in solutions obtained by ANN-SOS approach for Case 2.

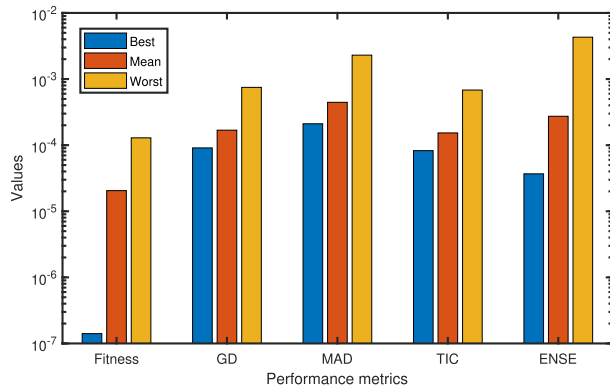
$$\begin{aligned} &+ \frac{7.99995174840100}{1 + e^{-(-3.21426240214401 * X - 6.72161898888413)}} \\ &+ \frac{1.87955662156705}{1 + e^{-(-3.34214216015950 * X - 7.03789761598474)}} \\ &+ \frac{4.20112535133326}{1 + e^{-(-2.66339337359687 * X - 4.66745040374569)}} \\ &- \frac{0.0128104320933259}{1 + e^{-(-6.06477983034726 * X - 6.90897301935497)}} \\ &+ \frac{0.667318004905647}{1 + e^{-(-7.99959571106342 * X - 4.92613085857431)}} \\ &+ \frac{7.96045657466436}{1 + e^{-(-1.48132135558938 * X - 4.80074737155237)}} \\ &+ \frac{3.56631816342962}{1 + e^{-(-2.43360164563693 * X - 7.99879499067904)}} \end{aligned}$$



(a) Performance indicators for n=0.



(b) Performance indicators for n=1.



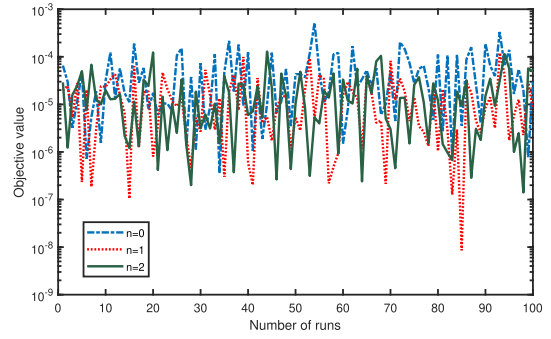
(c) Performance indicators for n=2.

FIGURE 17. Performance indicators obtained by ANN-SOS approach for Case 2.

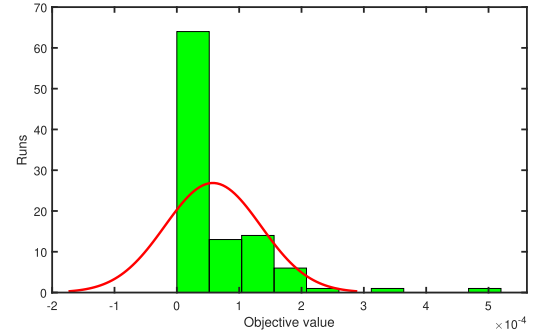
$$+ \frac{0.682533958309906}{1 + e^{-(4.16828048633773 * X + 7.77987581001960)}} \quad (46)$$

Solution for trapezoidal profile (n = 1):

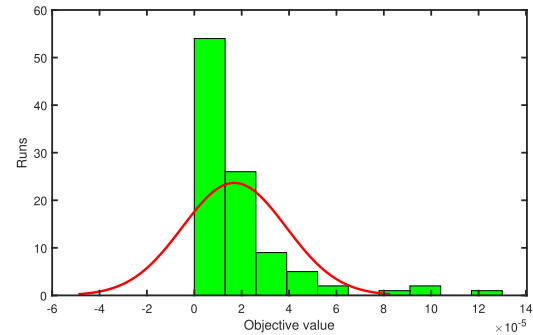
$$\hat{\theta}_{C2(n=1)} = \frac{3.37861901041481}{1 + e^{-(1.51017013736570 * X - 4.25606574556345)}} + \frac{-0.104576991031446}{1 + e^{-(8.06597495742229 * X - 5.25158549466864)}} + \frac{-4.93571726075515}{1 + e^{-(1.8293665577885 * X - 6.20954497145383)}} + \frac{0.654609312931376}{1 + e^{-(3.07052280824493 * X + 5.45138383342858)}}$$



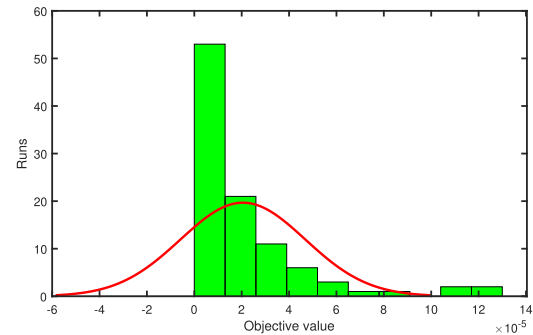
(a) Fitness values for case 2.



(b) Fitness values for n=0.



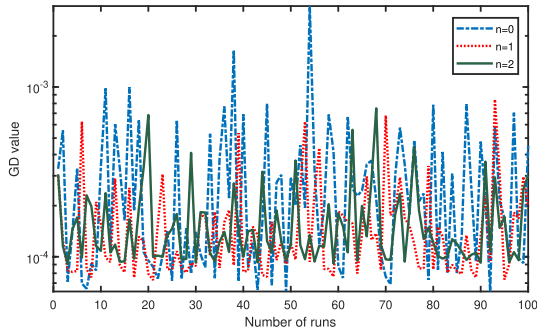
(c) Fitness values for n=1.



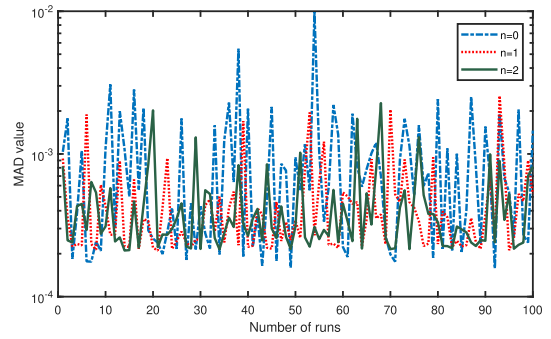
(d) Fitness values for n=2.

FIGURE 18. Results in terms of fitness values obtained by ANN-SOS approach for Case 2.

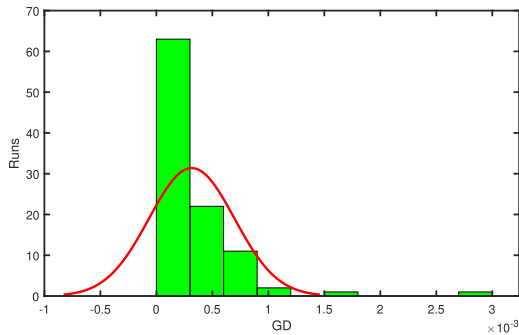
$$+ \frac{-1.79020558320029}{1 + e^{-(2.40440387386212 * X - 4.37785057125410)}} + \frac{6.10284604160929}{1 + e^{-(2.90024034371422 * X - 4.74092325506649)}} + \frac{9.97166023285747}{1 + e^{-(1.94874276510895 * X - 5.25387936782479)}}$$



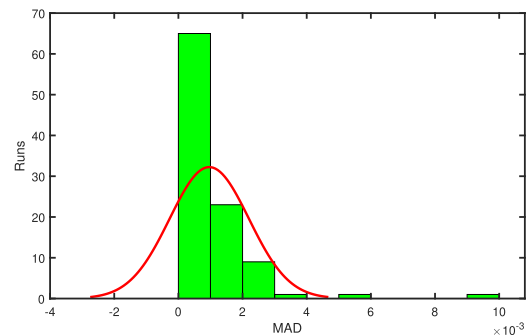
(a) GD values for case 2.



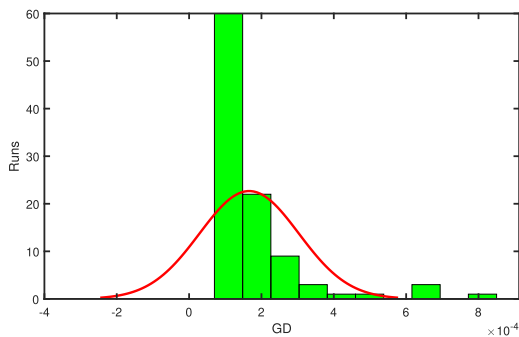
(a) MAD values for case 2.



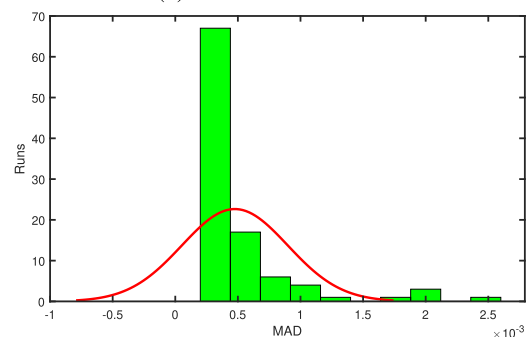
(b) GD values for n=0.



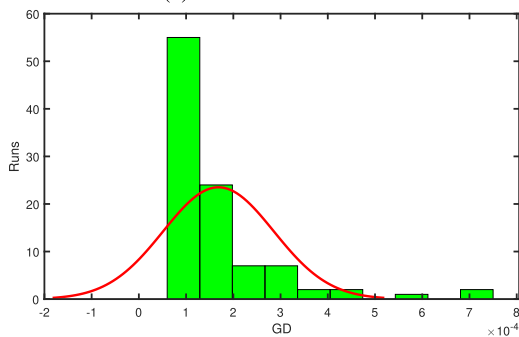
(b) MAD values for n=0.



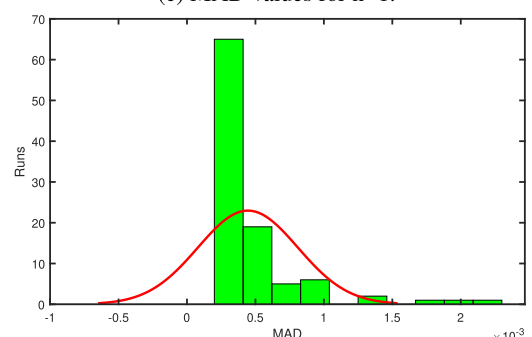
(c) GD values for n=1.



(c) MAD values for n=1.



(d) GD values for n=2.



(d) MAD values for n=2.

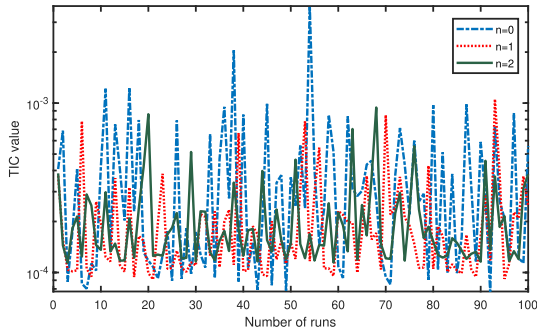
FIGURE 19. Results in terms of GD values obtained by ANN-SOS approach for Case 2.

FIGURE 20. Results in terms of MAD values obtained by ANN-SOS approach for Case 2.

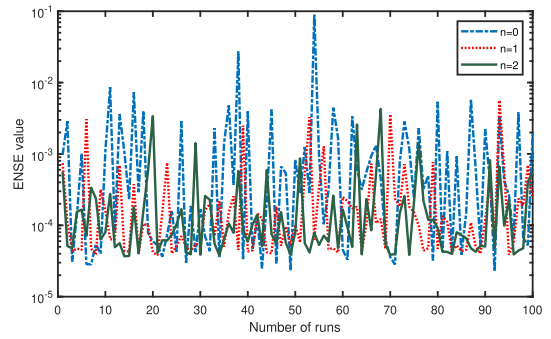
$$\begin{aligned}
 & \frac{-0.0987938321289193}{1 + e^{-(-7.51381126423256 * X - 4.71577014681001)}} \\
 & + \frac{9.62737324205448}{1 + e^{-(2.59491091377733 * X - 9.99582145127654)}} \\
 & + \frac{0.614568721878469}{1 + e^{-(-9.99715514112820 * X - 7.12145823149072)}}. \quad (47)
 \end{aligned}$$

Solution for concave parabolic profile (n = 2):

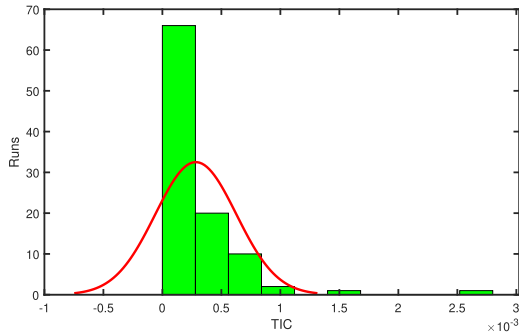
$$\begin{aligned}
 \hat{\theta}_{C2(n=2)} &= \frac{0.242952601477876}{1 + e^{-(0.170769550729980 * X - 1.96149910357359)}}
 \end{aligned}$$



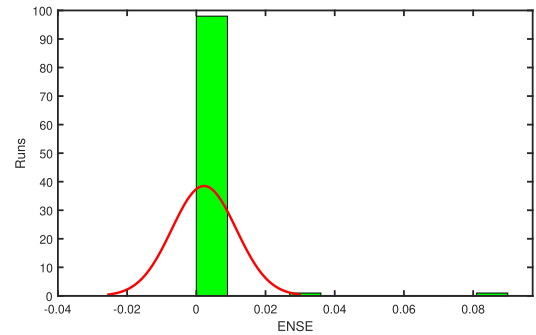
(a) TIC values for case 2.



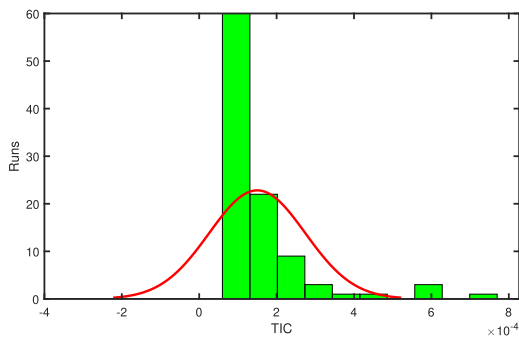
(a) ENSE values for case 2.



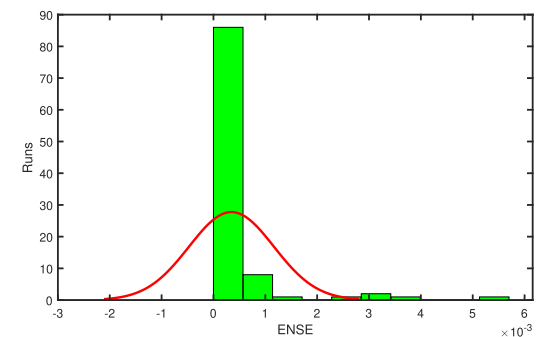
(b) TIC values for n=0.



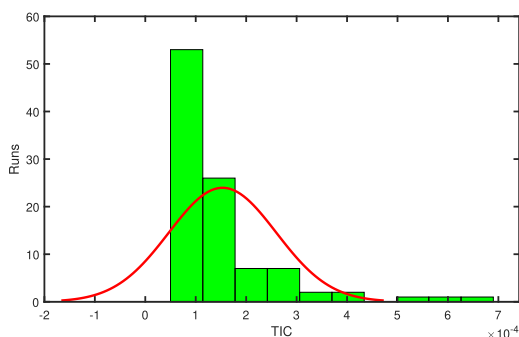
(b) ENSE values for n=0.



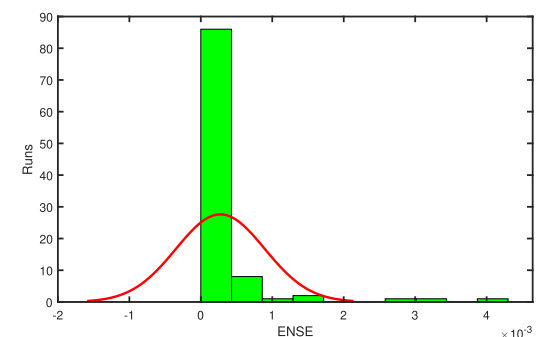
(c) TIC values for n=1.



(c) ENSE values for n=1.



(d) TIC values for n=2.



(d) ENSE values for n=2.

FIGURE 21. Results in terms of TIC values obtained by ANN-SOS approach for Case 2.

FIGURE 22. Results in terms of ENSE values obtained by ANN-SOS approach for Case 2.

$$\begin{aligned}
 & \frac{0.266926563180618}{1 + e^{-(-9.98712895736556 * X - 7.20455267949591)}} \\
 & \frac{-3.80287817476829}{1 + e^{-(-1.13526918743326 * X - 2.52082621032299)}} \\
 & \frac{-9.99372027984724}{1 + e^{-(-3.27929766074586 * X - 8.25440647158961)}}
 \end{aligned}$$

$$\begin{aligned}
 & \frac{-7.74374571493655}{1 + e^{-(0.424675253812910 * X - 9.82832804440684)}} \\
 & \frac{-0.759618870894774}{1 + e^{-(-1.63624150724474 * X - 3.52861174050779)}} \\
 & \frac{2.39687891613306}{1 + e^{-(-1.78168798314758 * X - 1.51263644815141)}}
 \end{aligned}$$

$$\begin{aligned}
& + \frac{0.00622520230216788}{1 + e^{-(-4.54126336673020 * X + 2.18350336676046)}} \\
& + \frac{0.621058810095202}{1 + e^{-(-3.54323075636798 * X - 6.30068235691339)}} \\
& + \frac{3.45031966347335}{1 + e^{-(-0.580714491848014 * X - 1.55883409039987)}}. \quad (48)
\end{aligned}$$

For the trapezoidal profile, the absolute minimum errors lie between 10^{-05} to 10^{-08} , and the mean errors are about 10^{-04} . The absolute minimum errors in the solutions for concave parabolic profile range from 10^{-05} to 10^{-07} , and the mean errors are in the range of 10^{-03} to 10^{-04} . The best, mean, and worst absolute errors in the solutions are also given in FIGURE (16). To check the accuracy of the solutions obtained by the ANN-SOS algorithm, the performance metrics are also evaluated. The numerical results for performance metrics are given in TABLES (14) and (12). From TABLE (14), we can see that the generational distance between the exact solution and approximate solutions at each point in the interval $[0, 1]$ range from 10^{-03} to 10^{-05} which shows that the exact and approximate solutions are very close to each other. The values of performance metric MAD range from 10^{-03} to 10^{-04} . In TABLE (12), the values of performance metrics TIC and ENSE are given. The values of TIC and ENSE range from 10^{-03} to 10^{-05} and 10^{-02} to 10^{-05} respectively. Bar graphs for best, mean, and worst values of fitness function and performance metrics are also given in FIGURE (17). The histogram plots for fitness values are given in FIGURE (18). The FIGURE shows that for rectangular profiles more than 70% of the fitness values are less than 10^{-05} and for trapezoidal and concave parabolic profiles more than 90% are less than 10^{-05} . The histogram plots for GD values are given in FIGURE (19). It is clear from the plots that for rectangular profile, more than 90% values are less than 10^{-04} , and for trapezoidal and concave parabolic profiles, most of the values are between 10^{-04} to 10^{-05} . In FIGURE (20), histograms for values of MAD are presented and it clear that most of the values are between 10^{-03} to 10^{-05} . TIC values are plotted in FIGURE (21) and we can see that most of the values are between 10^{-03} to 10^{-05} . FIGURE (22) shows the values of ENSE and most of the values are between 10^{-02} to 10^{-05} . Convergence analysis for case 2 is given in TABLE (15). It is observed from TABLES (9-11) and FIGURE (15a, 15b, and 15c) that in case 2 temperature distribution ranges between 0.78855 to 1 (for rectangular profile), 0.771386 to 1 (for trapezoidal profile), and 0.761446 to 1 (for concave parabolic profile). Moreover, for a better understanding of frequency plots, we have presented TABLE 15. In this TABLE, we have given success rates of different thresholds for fitness values, GD, MAD, TIC, and ENSE. Our solutions and errors in solutions are compared with solutions calculated in [38], see TABLES (9-11). For each profile, the ANN-SOS algorithm is successful in getting solutions to better quality with minimum errors.

VI. CONCLUSION

In this research, we have considered a mathematical model of longitudinal heat exchangers (fins). It involves a complex

ODE with boundary values. Our key findings are concluded as follows:

- We have analyzed a mathematical model which represents the temperature profiles of longitudinal fins with concave parabolic, rectangular, and trapezoidal shapes, see Section 2 and FIGURE 2.
- A new neuroevolutionary is proposed in which we have combined the strengths of Artificial Neural Networks (ANNs) and the Symbiotic Organism Search (SOS) algorithm. It is named as ANN-SOS algorithm, see Section 3, FIGURES 1 and 3.
- We have divided our problem into two main scenarios, and six sub-problem. Case 1 and 2 are different in terms of thermal conductivity parameter (A), convective conduction parameter (N_c), exponent of convective heat transfer (m), and radiation-conduction parameter (N_r). Moreover, in sub-problems for each case, we are considering three different designs (rectangular, trapezoidal, and concave parabolic) for $n = 0, 1, 2$ respectively, see FIGURES 2, and 4.
- Performance indicators like generational distance (GD), Root mean squared errors (RMSE), absolute errors (AE), Mean absolute deviation (MAD), Nash–Sutcliffe efficiency (NSE), error in Nash–Sutcliffe efficiency (ENSE) are calculated for all six problems to validate the efficacy of our approach. Our results are in strong agreement with state-of-the-art solutions.
- Series solutions for all six problems are presented in Equations (37-39), and (46-48). These solutions may be used by researchers to reproduce our results for further studies.
- Experimental results obtained by the ANN-SOS algorithm are tabulated in TABLES (2-8) for case 1, and in TABLES (9-15) for case 2. These TABLES include numerical values of best weights, absolute errors in our solutions, mean and standard deviations in absolute errors, GD, MAD, TIC, and ENSE values. It is evident from these TABLES that the ANN-SOS algorithm is robust and accurate.
- Graphical illustration of our experimental outcome is presented in this paper. Results for case 1 are elaborated in FIGURES (5-13), and case 2 is depicted in FIGURES (14-22).
 - From FIGURES 6 and 15 we observed that ANN-SOS algorithm has produced results of high quality and are overlapping with state-of-the-art solutions.
 - Absolute errors for $n = 0, 1, 2$ in both cases are lower and points to the efficiency and accuracy of ANN-SOS algorithm, see FIGURE 7, 16.
 - Frequency charts with normal distribution fits are given for absolute errors, GD, MAD, TIC, and ENSE values. See FIGURES (8-13) and (17-22). These graphs illustrate that ANN-SOS algorithm is stable and can handle problems of real applications.

- We have plotted values obtained through 100 experiments to validate our claims further. See sub-FIGURES (a) in (9-13), and (18-22).

- Different activation functions may be used to construct ANN series solutions.

All these analyses suggest that the ANN-SOS algorithm has calculated solutions of better quality, and it can solve real application problems having no prior information about its objective functions. ANN-SOS algorithm may be used to solve higher-order ODEs involving fractional derivatives.

REFERENCES

- [1] G. Domairry and M. Fazeli, "Homotopy analysis method to determine the fin efficiency of convective straight fins with temperature-dependent thermal conductivity," *Commun. Nonlinear Sci. Numer. Simul.*, vol. 14, no. 2, pp. 489–499, Feb. 2009.
- [2] Z.-Y. Lee, "Method of bilaterally bounded to solution Blasius equation using particle swarm optimization," *Appl. Math. Comput.*, vol. 179, no. 2, pp. 779–786, Aug. 2006.
- [3] S. B. Coşkun and M. T. Atay, "Analysis of convective straight and radial fins with temperature-dependent thermal conductivity using variational iteration method with comparison with respect to finite element analysis," *Math. Problems Eng.*, vol. 2007, pp. 1–15, Dec. 2007.
- [4] S. B. Coşkun and M. T. Atay, "Fin efficiency analysis of convective straight fins with temperature dependent thermal conductivity using variational iteration method," *Appl. Thermal Eng.*, vol. 28, nos. 17–18, pp. 2345–2352, Dec. 2008.
- [5] C.-H. Chiu and C.-K. Chen, "Application of the decomposition method to thermal stresses in isotropic circular fins with temperature-dependent thermal conductivity," *Acta Mechanica*, vol. 157, nos. 1–4, pp. 147–158, Mar. 2002.
- [6] C. Arslanturk, "Correlation equations for optimum design of annular fins with temperature dependent thermal conductivity," *Heat Mass Transf.*, vol. 45, no. 4, pp. 519–525, Feb. 2009.
- [7] J. K. Zhou, *Differential Transformation and Its Applications for Electrical Circuits*. Wuhan, China: Huazhong Univ. Press (in Chinese), 1986, pp. 1279–1289.
- [8] M. M. Rashidi, N. Laraq, and S. M. Sadri, "A novel analytical solution of mixed convection about an inclined flat plate embedded in a porous medium using the DTM-Padé," *Int. J. Thermal Sci.*, vol. 49, no. 12, pp. 2405–2412, Dec. 2010.
- [9] B. Kundu and D. Barman, "Analytical study on design analysis of annular fins under dehumidifying conditions with a polynomial relationship between humidity ratio and saturation temperature," *Int. J. Heat Fluid Flow*, vol. 31, no. 4, pp. 722–733, Aug. 2010.
- [10] H. Yaghoobi and M. Torabi, "The application of differential transformation method to nonlinear equations arising in heat transfer," *Int. Commun. Heat Mass Transf.*, vol. 38, no. 6, pp. 815–820, Jul. 2011.
- [11] M. Torabi, H. Yaghoobi, and A. Fereidoon, "Application of differential transformation method and Padé approximant for the Glauert-jet problem," *Recent Patents Mech. Eng.*, vol. 5, no. 2, pp. 150–155, Apr. 2012.
- [12] H.-P. Chu and C.-L. Chen, "Hybrid differential transform and finite difference method to solve the nonlinear heat conduction problem," *Commun. Nonlinear Sci. Numer. Simul.*, vol. 13, no. 8, pp. 1605–1614, Oct. 2008.
- [13] H.-P. Chu and C.-Y. Lo, "Application of the hybrid differential transform-finite difference method to nonlinear transient heat conduction problems," *Numer. Heat Transf., A, Appl.*, vol. 53, no. 3, pp. 295–307, Oct. 2007.
- [14] H.-S. Peng and C.-L. Chen, "Hybrid differential transformation and finite difference method to annular fin with temperature-dependent thermal conductivity," *Int. J. Heat Mass Transf.*, vol. 54, nos. 11–12, pp. 2427–2433, May 2011.
- [15] M. Torabi, H. Yaghoobi, and K. Boubaker, "Accurate solution for motion of a spherical solid particle in plane couette newtonian fluid mechanical flow using HPM-Padé approximant and the Boubaker polynomials expansion scheme BPES," *Int. J. Heat Mass Transf.*, vol. 58, nos. 1–2, pp. 224–228, Mar. 2013.
- [16] S. Yalçınbaş and M. Sezer, "The approximate solution of high-order linear Volterra-Fredholm integro-differential equations in terms of Taylor polynomials," *Appl. Math. Comput.*, vol. 112, nos. 2–3, pp. 291–308, Jun. 2000.
- [17] P. Darania and A. Ebadian, "Development of the Taylor expansion approach for nonlinear integro-differential equations," *Int. J. Contemp. Math. Sci.*, vol. 1, no. 14, pp. 651–664, 2006.
- [18] P. Darania and A. Ebadian, "A method for the numerical solution of the integro-differential equations," *Appl. Math. Comput.*, vol. 188, no. 1, pp. 657–668, 2007.
- [19] P. Darania and K. Ivaz, "Numerical solution of nonlinear Volterra-Fredholm integro-differential equations," *Comput. Math. Appl.*, vol. 56, no. 9, pp. 2197–2209, 2008.
- [20] P. Roul and P. Meyer, "Numerical solutions of systems of nonlinear integro-differential equations by homotopy-perturbation method," *Appl. Math. Model.*, vol. 35, no. 9, pp. 4234–4242, Sep. 2011.
- [21] M. Torabi and H. Yaghoobi, "Novel solution for acceleration motion of a vertically falling spherical particle by HPM-Padé approximant," *Adv. Powder Technol.*, vol. 22, no. 5, pp. 674–677, Sep. 2011.
- [22] H. Yaghoobi and M. Torabi, "Novel solution for acceleration motion of a vertically falling non-spherical particle by VIM-Padé approximant," *Powder Technol.*, vols. 215–216, pp. 206–209, Jan. 2012.
- [23] I. H. Osman and G. Laporte, "Metaheuristics: A bibliography," *Ann. Oper. Res.*, vol. 63, pp. 511–623, Oct. 1996.
- [24] F. W. Glover and G. A. Kochenberger, *Handbook of Metaheuristics*, vol. 57. Cham, Switzerland: Springer, 2006.
- [25] X.-S. Yang, *Nature-Inspired Metaheuristic Algorithms*. York, U.K.: Luniver Press, 2010.
- [26] X.-S. Yang, *Engineering Optimization: An Introduction with Metaheuristic Applications*. Hoboken, NJ, USA: Wiley, 2010.
- [27] A. Khan, M. Sulaiman, H. Alhakami, and A. Alhindi, "Analysis of oscillatory behavior of heart by using a novel neuroevolutionary approach," *IEEE Access*, vol. 8, pp. 86674–86695, 2020.
- [28] W. Waseem, M. Sulaiman, A. Alhindi, and H. Alhakami, "A soft computing approach based on fractional order DPSO algorithm designed to solve the corneal model for eye surgery," *IEEE Access*, vol. 8, pp. 61576–61592, 2020.
- [29] A. H. Bukhari, M. A. Z. Raja, M. Sulaiman, S. Islam, M. Shoaib, and P. Kumam, "Fractional neuro-sequential ARFIMA-LSTM for financial market forecasting," *IEEE Access*, vol. 8, pp. 71326–71338, 2020.
- [30] W. Waseem, M. Sulaiman, S. Islam, P. Kumam, R. Nawaz, M. A. Z. Raja, M. Farooq, and M. Shoaib, "A study of changes in temperature profile of porous fin model using cuckoo search algorithm," *Alexandria Eng. J.*, vol. 59, no. 1, pp. 11–24, Feb. 2020.
- [31] M. Sulaiman, I. Samiullah, A. Hamdi, and Z. Hussain, "An improved whale optimization algorithm for solving multi-objective design optimization problem of PFHE," *J. Intell. Fuzzy Syst.*, vol. 37, no. 3, pp. 3815–3828, Oct. 2019.
- [32] A. H. Bukhari, M. Sulaiman, S. Islam, M. Shoaib, P. Kumam, and M. A. Z. Raja, "Neuro-fuzzy modeling and prediction of summer precipitation with application to different meteorological stations," *Alexandria Eng. J.*, vol. 59, no. 1, pp. 101–116, Feb. 2020.
- [33] M. Sulaiman, S. Ahmad, J. Iqbal, A. Khan, and R. Khan, "Optimal operation of the hybrid electricity generation system using multiverse optimization algorithm," *Comput. Intell. Neurosci.*, vol. 2019, pp. 1–12, Mar. 2019.
- [34] M. Sulaiman, A. Salhi, B. I. Selamoglu, and O. B. Kirikchi, "A plant propagation algorithm for constrained engineering optimisation problems," *Math. Problems Eng.*, vol. 2014, pp. 1–10, May 2014.
- [35] M. Sulaiman and A. Salhi, "A seed-based plant propagation algorithm: The feeding station model," *Sci. World J.*, vol. 2015, pp. 1–16, Mar. 2015.
- [36] M. Sulaiman, M. Sulaman, A. Hamdi, and Z. Hussain, "The plant propagation algorithm for the optimal operation of directional over-current relays in electrical engineering," *Mehran Univ. Res. J. Eng. Technol.*, vol. 39, no. 2, pp. 223–236, Apr. 2020.
- [37] M. Sulaiman, A. Salhi, A. Khan, S. Muhammad, and W. Khan, "On the theoretical analysis of the plant propagation algorithms," *Math. Problems Eng.*, vol. 2018, pp. 1–8, Mar. 2018.
- [38] A. Sadollah, H. Eskandar, D. G. Yoo, and J. H. Kim, "Approximate solving of nonlinear ordinary differential equations using least square weight function and Metaheuristic algorithms," *Eng. Appl. Artif. Intell.*, vol. 40, pp. 117–132, Apr. 2015.
- [39] A. Hassan, S.-U.-I. Ahmad, M. Kamran, A. Illahi, and R. M. A. Zahoor, "Design of cascade artificial neural networks optimized with the memetic computing paradigm for solving the nonlinear Bratu system," *Eur. Phys. J. Plus*, vol. 134, no. 3, p. 122, Mar. 2019.

- [40] W. Arloff, K. R. B. Schmitt, and L. J. Venstrom, "A parameter estimation method for stiff ordinary differential equations using particle swarm optimisation," *Int. J. Comput. Sci. Math.*, vol. 9, no. 5, pp. 419–432, 2018.
- [41] N. Yadav, A. Yadav, M. Kumar, and J. H. Kim, "An efficient algorithm based on artificial neural networks and particle swarm optimization for solution of nonlinear Troesch's problem," *Neural Comput. Appl.*, vol. 28, no. 1, pp. 171–178, Jan. 2017.
- [42] I. Th. Famelis, A. Alexandridis, and C. Tsitouras, "A highly accurate differential evolution-particle swarm optimization algorithm for the construction of initial value problem solvers," *Eng. Optim.*, vol. 50, no. 8, pp. 1364–1379, Aug. 2018.
- [43] M. A. Z. Raja and S.-U.-I. Ahmad, "Numerical treatment for solving one-dimensional Bratu problem using neural networks," *Neural Comput. Appl.*, vol. 24, nos. 3–4, pp. 549–561, Mar. 2014.
- [44] B. O. Fatimah, W. A. Senapon, and A. M. Adebowale, "Solving ordinary differential equations with evolutionary algorithms," *Open J. Optim.*, vol. 4, no. 3, p. 69, 2015.
- [45] M. A. Z. Raja, F. H. Shah, and M. I. Syam, "Intelligent computing approach to solve the nonlinear Van der Pol system for heartbeat model," *Neural Comput. Appl.*, vol. 30, no. 12, pp. 3651–3675, Dec. 2018.
- [46] N. N. El-Emam and R. H. Al-Rabeh, "An intelligent computing technique for fluid flow problems using hybrid adaptive neural network and genetic algorithm," *Appl. Soft Comput.*, vol. 11, no. 4, pp. 3283–3296, Jun. 2011.
- [47] S. Wen, W. Liu, Y. Yang, T. Huang, and Z. Zeng, "Generating realistic videos from keyframes with concatenated GANs," *IEEE Trans. Circuits Syst. Video Technol.*, vol. 29, no. 8, pp. 2337–2348, Aug. 2019.
- [48] M. Dong, S. Wen, Z. Zeng, Z. Yan, and T. Huang, "Sparse fully convolutional network for face labeling," *Neurocomputing*, vol. 331, pp. 465–472, Feb. 2019.
- [49] S. Wen, M. Dong, Y. Yang, P. Zhou, T. Huang, and Y. Chen, "End-to-end detection-segmentation system for face labeling," *IEEE Trans. Emerg. Topics Comput. Intell.*, early access, Nov. 6, 2019, doi: 10.1109/TETCI.2019.2947319.
- [50] Y. Cao, S. Wang, Z. Guo, T. Huang, and S. Wen, "Synchronization of memristive neural networks with leakage delay and parameters mismatch via event-triggered control," *Neural Netw.*, vol. 119, pp. 178–189, Nov. 2019.
- [51] S. Wang, Y. Cao, T. Huang, Y. Chen, and S. Wen, "Event-triggered distributed control for synchronization of multiple memristive neural networks under cyber-physical attacks," *Inf. Sci.*, vol. 518, pp. 361–375, May 2020.
- [52] S. Chakraverty and S. Mall, "Single layer Chebyshev neural network model with regression-based weights for solving nonlinear ordinary differential equations," *Evol. Intell.*, pp. 1–8, Mar. 2020.
- [53] Z. Sabir, H. A. Wahab, M. Umar, M. G. Sakar, and M. A. Z. Raja, "Novel design of Morlet wavelet neural network for solving second order Lane-Emden equation," *Math. Comput. Simul.*, vol. 172, pp. 1–14, Jun. 2020.
- [54] C. Nwankpa, W. Ijomah, A. Gachagan, and S. Marshall, "Activation functions: Comparison of trends in practice and research for deep learning," 2018, *arXiv:1811.03378*. [Online]. Available: <http://arxiv.org/abs/1811.03378>
- [55] A. Sadollah, Y. Choi, D. G. Yoo, and J. H. Kim, "Metaheuristic algorithms for approximate solution to ordinary differential equations of longitudinal fins having various profiles," *Appl. Soft Comput.*, vol. 33, pp. 360–379, Aug. 2015.
- [56] M.-Y. Cheng and D. Prayogo, "Symbiotic organisms search: A new metaheuristic optimization algorithm," *Comput. Struct.*, vol. 139, pp. 98–112, Jul. 2014.



ASHFAQ AHMAD received the B.S. degree in mathematics from Islamia College Peshawar, in 2015, the M.Phil. degree in mathematics from Abdul Wali Khan University Mardan, Pakistan, in 2018, where he is currently pursuing the Ph.D. degree in mathematics. His research interests include optimization algorithms, real world problems, bio-inspired algorithms, artificial neural networks, and energy management.



MUHAMMAD SULAIMAN received the B.Sc. degree from the University of Peshawar, in 2004, the M.Sc. and M.Phil. degrees in mathematics from Quaid-e-Azam University, Islamabad, Pakistan, in 2007 and 2009, respectively, and the Ph.D. degree in mathematics from the University of Essex, U.K., in 2015. From 2009 to 2016, he was a Lecturer in mathematics with the Abdul Wali Khan University Mardan, Pakistan, where he has been an Assistant Professor with the Department of Mathematics since February 2016. He is the author of two book chapters and more than 25 research articles. His research interests include mathematical optimization techniques, global optimization, and evolutionary algorithms, heuristics, metaheuristics, multi-objective optimization, design engineering optimization problems, structural engineering optimization problems, linear programming, linear and non-linear least squares optimization problems, evolutionary algorithms, nature-inspired metaheuristics, artificial neural networks, and differential equations. He is an Associate Editor of the *Journal COJ Reviews and Research* and the *SCIREA Journal of Mathematics*.



AHMAD ALHINDI (Member, IEEE) received the B.Sc. degree in computer science from Umm al-Qura University (UQU), Makkah, Saudi Arabia, in 2006, and the M.Sc. degree in computer science and the Ph.D. degree in computing and electronic systems from the University of Essex, Colchester, U.K., in 2010 and 2015, respectively. He is currently an Assistant Professor of artificial intelligence (AI) with the Computer Science Department and a Researcher of CIADA, UQU. His current research interests include evolutionary multi-objective optimization and machine learning techniques. He is also involved in AI algorithms, focusing particularly on machine learning, and optimization with a willingness to implement them in the context of decision making and solving combinatorial problems in real-world projects.



ABDULAH JEZA ALJOHANI (Member, IEEE) received the B.Sc. (Eng.) degree in electronics and communication engineering from King Abdulaziz University, Jeddah, Saudi Arabia, in 2006, and the M.Sc. (Hons.) and Ph.D. degrees in wireless communication from the University of Southampton, Southampton, U.K., in 2010 and 2016, respectively. He is currently an Assistance Professor with the Department of Electrical and Computer Engineering, King Abdulaziz University, Jeddah, Saudi Arabia. He is also associated with the Center of Excellence in Intelligent Engineering Systems. His research interests include convex optimization, joint source/channel coding, distributed source coding, the IoT, channel coding, cooperative communications, and MIMO systems. He awarded his Ph.D. degree with no corrections.

...